AD 255 584

A STUDY OF RECONNAISSANCE DATA FROM A BOOST-GLIDE VEHICLE

TR NO. 61-51
REPORT NO. CM-1418-G-1 69 100 (NOad-7316)
FEBRUARY 15, 1961
CONTRACT NO. AF30(602)-2183
ROME AIR DEVELOPMENT CENTER

CORNELL AERONAUTICAL LABORATORY, INC.
OF CORNELL UNIVERSITY, BUFFALO 21, N. Y.

COPY NO. ___
OF 65 COPIES

A STUDY OF RECONNAISSANCE DATA FROM A BOOST-GLIDE VEHICLE

TR NO. 61-51
REPORT NO. CM-1418-G-1
FEBRUARY 15, 1961
CONTRACT NO. AF30(602)-2183
ROME AIR DEVELOPMENT CENTER

prepared by Paul G. Roetling
Paul G. Roetling
project engineer

approved by E. H. Gerber
E. H. Gerber
head, system synthesis section

approved by D. A. Kahn
D. A. Kahn
head, systems research department

CORNELL AERONAUTICAL LABORATORY, INC.
OF CORNELL UNIVERSITY, BUFFALO 21, N. Y.

ACKNOWLEDGEMENTS

The investigation described in this report was performed under the direction of Mr. J. A. Stringham and Mr. L. D. Sinnamon of RADC. The latter was the Air Force Project Engineer.

In the Cornell Aeronautical Laboratory, Inc., contributors to the project, in addition to the author, were:

Ralph Berggren
Joseph Bomstein
Stephen Graczyk
Roger Haas
Paul McKowen

FOREWORD

This study was initiated by the Reconnaissance Charting Branch of the Intelligence Laboratory as a part of the Air Force program to develop a target location and charting capability compatible with future weapon systems. Specifically, the purpose of this study was to investigate the unique possibilities presented by the inclusion of different kinds of sensors in a high-performance boost-glide type of vehicle. However, to keep the work within the limitations of the contract, only the various combinations of panoramic photography and side scan radar were considered. Because of the lack of the fundamental experiments that are needed for an adequate determination of the expected atmospheric effects, that portion of the work was only briefly covered.

Two important conclusions were drawn from this work:

1. To match different sensor records from the high altitudes under consideration, the establishment of a stereo model or even the rectification of the images would not permit registration of the images, because of the difference in direction of relief displacement, unless a local datum and techniques for forced matching of recognizable points were used.

2. Before a choice is made for a multi-sensor collection system, many factors need to be considered, e.g., since radar is essentially independent of stabilization and radar stereo is only slightly dependent upon the relative positions of the two sensors, a radar system will outperform the photographic system if navigation and stabilization errors are large whereas, at low altitudes, stabilization errors do not appreciably affect the systems and photographic sensors can be used. At higher altitudes, stabilization errors can dominate a photographic system. Implied in these conclusions is the fact that resolution is not a limiting factor.

A few conditions for each parametric equation were used as a basis for the above conclusions as presented in this report. Because it was not advisable to examine all the possible conditions, those of greatest interest to an individual may not have been included. If the necessary information is not found in this document, it may be possible to utilize the computer program to generate the information.

This work has resulted in interesting conclusions that should be taken into consideration during the configuration of a vehicle to be used for multi-sensor target location or charting.

This document presents the results of a scientific investigation. It is hoped that it will stimulate interest in the problem under consideration and will serve as an indication of our interest. Comments on this work are invited and should be addressed to the contract scientist.

Lynwood D. Sinnamon, Jr.
Physical Scientist
ATTN: RCWICC
Rome Air Development Center
Griffiss AFB, New York

March 1961

ABSTRACT

Target location and charting using data acquired by boost-glide type vehicles are investigated. Particular emphasis is placed on two aspects of the problem; the use of multiple sensors, and atmospheric effects.

The possibility of improving target location accuracy by using combinations of different sensor types is investigated. A parametric analysis provides error contributions due to various sources as functions of altitude, target offset, and sensor separation in 3-D location systems. Trade-offs between various systems are presented.

Atmospheric effects are described analytically. Where experimental data could be obtained, various refraction effects are evaluated numerically and plotted as a function of altitude.

TABLE OF CONTENTS

LIST OF ILLUSTRATIONS

LIST OF TABLES

LIST OF APPENDICES

SUMMARY

A one year study has been conducted during which two aspects of the problem of target location and charting from boost-glide type vehicles have been investigated. First, possible improvements in target location accuracy through the use of combinations of different sensor types were studied. Second, the atmosphere, a major source of image distortion and degradation, has been treated analytically, and a survey of present experimental data was conducted.

Target location accuracy was investigated by evaluating location errors for several combinations of sensors. Sensor altitude, target position, and sensor separation were varied parametrically. Measurement errors were varied, so that system trade-offs could be found as a function of improvement in sensors or other equipment (such as navigation systems). It is likely that a combination of radar and camera in a single vehicle can outperform either radar or photographic stereo target location systems singly, unless the base line for photographic triangulation is large (as in the case of convergent photography or photographs taken on separate flights, where side-lap is used). Radar systems are less affected by navigation and orientation errors than camera systems, and so improve relative to photographic methods as these errors increase.

As a by-product of this study, it was possible to estimate the accuracy with which images could be brought into registration for superposition. It was found that single sensor images contain relief displacements large enough to allow only coarse registration. Matching stereo models improves the situation, but auxiliary aids such as relative control points must be used if small target objects are to be registered.

Atmospheric refraction studies indicate that above 100,000 feet, in the boost-glide altitude regime, the major distortion and degradation is due to atmospheric turbulence. Present experimental data are insufficient to establish reliable values for parameters in the theoretical equations, so precise evaluation of atmospheric effects is not possible at this time.

It is recommended that further work be done on target location systems to determine the reduction of errors when least squares adjustment of data is used in conjunction with ground control. Atmospheric experimentation, especially in the area of turbulence, should be continued.

1. INTRODUCTION

The Cornell Aeronautical Laboratory, Inc., under contract AF30 (602)-2183 with the Rome Air Development Center, has studied problems of reconnaissance from boost-glide type vehicles. The contract covered one year at approximately a one man level of effort.

Such a study has many facets. Two choices are open if a relatively small study is to be conducted. Either many aspects may be investigated in cursory fashion, or a few may be more thoroughly studied. With the agreement of the sponsoring agency this Laboratory chose the second alternative, with study effort being concentrated on the problems of target location tion using multiple sensors and atmospheric optical effects.

The question which arises with respect to target location and charting is: Can point location accuracy be improved by using combinations of sensors for location purposes? It is reasonable to expect that a combination of camera and radar might outperform either sensor used separately, since the camera provides directional data while the radar yields accurate range measurements. The target location accuracy study described in this report shows the conditions under which each sensor combination can be used to best advantage. The problems of mensuration are considered, with the assumption that targets are identifiable. Although the identification problem is not directly treated, this same study also provides data concerning the possibility of superimposing images from different sensors.

The atmosphere is, of course, a major source of image degradation and distortion in boost-glide reconnaissance. The study of the atmosphere is essentially a review of the state-of-the-art of this field. Refraction is treated in terms of the various sources of steady and fluctuating density gradients in the atmosphere. Results are presented, using the best available experimental data, which indicate the relative effect of these sources of image degradation and distortion.

The body of the report is divided into two parts. Part I describes the target location study while Part II is concerned with the atmosphere.

PART I

2. TARGET LOCATION

Target location may be considered in several stages of sophistication. The simplest form of target location consists of using a single sensor to obtain an image which contains the target. The range, or the direction, to the target is given by measurements of this image. The sensor altitude is then combined with these measurements to compute the target location with respect to the sensor. A knowledge of the sensor position with respect to the base of operations completes the target location. This simple system is plagued by two major errors, both due to the earth reference used. The simplest calculations assume a flat earth, and there is no way to account for terrain altitude variations in any case. The effects of earth curvature and terrain relief are calculated in the following section. Terrain relief errors alone are sufficiently large to warrant study of means to minimize their effect.

The errors due to using a reference datum can be eliminated by using data from two sensor images rather than one. "Stereo"* target location relies only on measurements on sensor images and a knowledge of the sensor position with respect to the base. Each sensor provides one or two measurements which aid in locating the target. Therefore, since the target must be located with respect to three coordinates, two** sensor images are needed. The mathematics of target location by this means, with an error analysis, is the subject of the major portion of Part I of this report. Various combinations of sensors are considered, indicating which combination provides the most accurate target location under various circumstances.

---

* "Stereo," as used in this report, means any system which locates targets by making use of two sensor records (at least) to provide three-dimensional location information. The term is not restricted to systems in which the images are viewed as a stereo model. Although this is 3-D target location, the term "stereo" was chosen to eliminate confusion between "3-D radar" which uses one sensor and "Stereo radar" which employs trilateration.

** One exception to this is 3-D radar, in which range, azimuth and elevation are all measured. However, elevation measurement errors are too large to seriously consider this system for target location from high altitude.

Any measurements which are available in excess of the required three may be used to reduce sensor measurement errors by least squares fitting of data. Thus, if one target appears on several images (such as happens in panoramic photography at large offset) the error expected from a simpler analysis could be reduced somewhat. Navigation errors can be reduced if several points on successive images can be used to extend ground control. Relative control points would reduce error contributions due to navigation measurements even if no absolute ground control was available. Again, this error reduction would involve a least squares fitting procedure. Such extensive mathematical analyses are beyond the scope of the present report. However, an introduction to this subject, showing that such procedures as have been developed for photography can be extended to include other types of sensors, is presented as an appendix to this report.

3. ERROR PROPAGATION IN NONSTEREO SYSTEMS

Two major errors arise when an attempt is made to locate a target by using a single sensor and a reference datum surface. The first contribution, which is negligible at low altitude, is the effect of earth curvature. This may, of course, be eliminated by the use of a curved reference datum. This effect is considered here only to the extent required to indicate when the simpler flat datum may be used.

The second error, similar in form to the first, is the effect of terrain relief. The location error due to terrain relief will be evaluated.

3.1 Earth Curvature Effect

Figure 3.1 illustrates the geometry of the situation for both camera and radar. The error in using a flat earth assumption can be computed as:

$$\text{Error} = E_c = NP - NP' \quad \text{, for camera} \qquad 3\text{-}1$$

$$E_R = NP - NP'' \quad \text{, for radar} \qquad 3\text{-}2$$

The distances NP, NP', NP'' can be computed from the figure, as:

$$NP' = H \tan\theta \qquad 3\text{-}3$$

$$NP = \alpha R_e \qquad 3\text{-}4$$

$$\alpha = \sin^{-1}\left[\left(1 + \frac{H}{R_e}\right)\sin\theta\right] - \theta \qquad 3\text{-}5$$

For the radar case:

$$(NP'')^2 = 2R_e^2\left[\left(1 + \frac{H}{R_e}\right)\right]\left[1 - \cos\left(\frac{NP}{R_e}\right)\right] \qquad 3\text{-}6$$

Since $\left(\frac{NP}{R_e}\right) = \alpha$ is an angle of a few degrees or less, 3-6 may be written:

$$NP'' = \sqrt{1 + \frac{H}{R_e}}\,(NP) \qquad 3\text{-}7$$

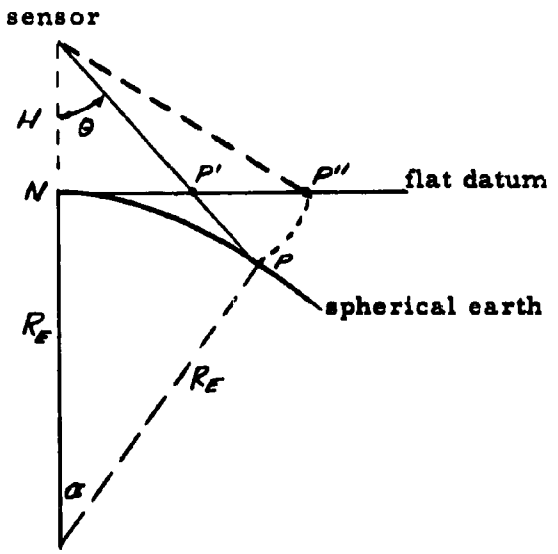

R_E = radius of earth
H = sensor altitude
N = nadir point
P = target point
P' = apparent target location (camera, flat datum)
P'' = apparent target location (radar, flat datum)
θ = field angle

Figure 3.1 EFFECT OF DATUM SURFACE ON TARGET LOCATION

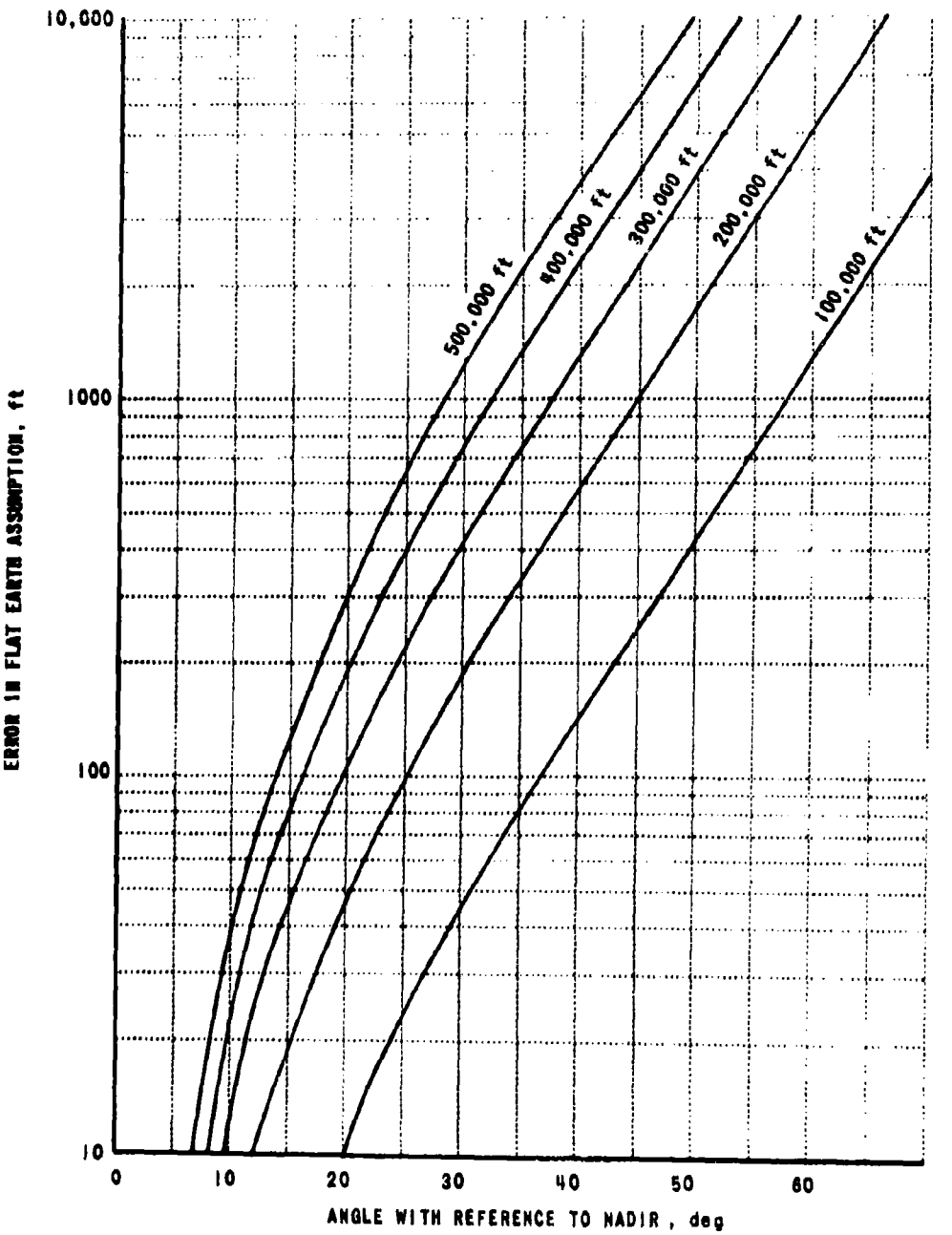

Figure 3.2 ERROR IN FLAT EARTH VS ANGLE TO OBJECT AT VARIOUS ALTITUDES FOR PHOTOGRAPHIC SYSTEM

Figure 3.2 shows the error in assuming a flat earth datum as a function of angle of the target away from nadir. Several altitudes are shown. Only errors for the photographic system are plotted, since Equation 3-7 shows that the error in the radar case is essentially a linear function of ground offset. It should be noted that photographic and radar effects are opposite in sign.

3.2 Terrain Relief

Figure 3.3 shows the effect of terrain relief. The pertinent equations relating to target location are given below. (It is assumed that the target is at a position at right angles to the flight line, directly to the side of the sensor platform.) The Y position of the target is computed as:

$$Y_R = \sqrt{R^2 - H^2} \qquad \text{for radar} \qquad 3\text{-}8$$

$$Y_c = H \tan\theta \qquad \text{for camera} \qquad 3\text{-}9$$

Relating these quantities, using Figure 3.3, assuming the target to be a height h above the terrain reference under the sensor:

$$\tan\theta = \frac{\sqrt{R^2 - (H-h)^2}}{(H-h)} = \sqrt{\frac{R^2}{(H-h)^2} - 1} \qquad 3\text{-}10$$

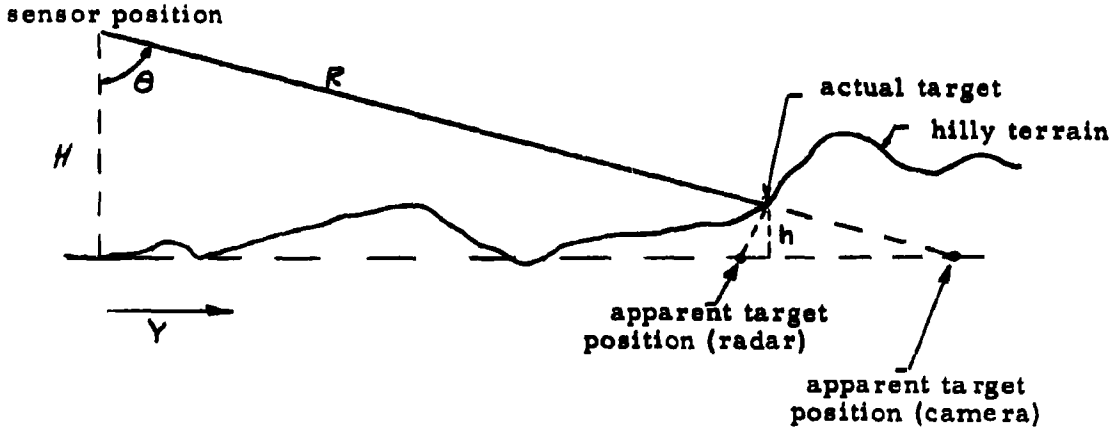

FIGURE 3.3 Effect of Terrain Relief on Target Location

A numerical example can be presented to indicate possible values of terrain relief errors. An angle within the field of both the camera and radar was chosen. The relief displacement for radar images increases for smaller angles away from nadir, while for photography the relief displacement is greater at larger angles. Table 3.1 summarizes the results.

Table 3.1 RELIEF DISPLACEMENT ERROR
(Using datum reference beneath sensor)

sensor altitude H	angle from nadir	relief	actual offset	relief displacement Photo	Radar
100 Kft	25°	1 Kft	46 Kft	+ 466 ft	-2140 ft
100 Kft	25°	100 Kft	46 Kft	+ 46.6 ft	- 214 ft
100 Kft	6°	1 Kft	10 Kft	+ 105 ft	(not
100 Kft	6°	100 Kft	10 Kft	+ 10.5 ft	applicable)

3.3 Results

It can be seen from Sections 3.1 and 3.2 that accurate target location cannot be achieved with nonstereo systems. Since the use of stereo would reduce target location errors, stereo systems will be considered in following sections.

If an attempt were made to bring a complete radar image and a photograph into registration, the images of some points would match, while others would be displaced relative to each other by the order of thousands of feet. Clearly only very large targets would still register under these conditions. Since large targets are already usually detectable on both images separately, there would be little advantage in combining them. Improvement could be achieved in regions where identifiable points allowed a local datum and scale to be used.

Assuming that only narrow field photographs are to be registered, the situation is better. If a target is near the center of one photograph, no appreciable relief displacement occurs. If the same target appears on a second photograph at 6° off axis, Table 3.1 shows that the target may be shifted ten to a hundred feet due to relief. If reliefs are in the order of 100 ft (gently rolling terrain), the 10 ft displacement is typical, in which case some value may be derived from superposition.

4. STEREO TARGET LOCATION ERROR ANALYSIS

As a basis for the parametric study to be considered, this section describes the basic target location equations for various sensor combinations and the error analysis which uses these equations. The results of this section are used in the following section which actually describes the parametric study. The equations will be developed, but not applied, in the present section.

It is assumed that a single target is to be located with respect to a coordinate system fixed at a known base. The target is to be located in all three dimensions, that is latitude, longitude and altitude (or equivalently x, y, z in a Cartesian system). Since no single sensor in one position provides the necessary data for 3-D target location, the problem must involve two sensors. These might be either the same sensor at different locations, or two different sensors. The problem, then is to determine a vector from the coordinate origin at a base to the target, by using partial information about two vectors from sensors to the target plus navigation vectors from the base to the sensors and orientation information about the sensors. Figure 4.1 illustrates the problem. The vector, $\vec{P}$, is to be determined.

Generally, $\vec{P}$ is determined by solving the following vector equation:

$$\vec{P} = \vec{S}_1 + \vec{R}_1 \qquad 4\text{-}1$$

where the navigation vector, $\vec{S}_1$ is known in base coordinates and $\vec{R}_1$ must be solved for by using:

$$\vec{R}_1 = \vec{S} + \vec{R}_2 \qquad 4\text{-}2$$

and

$$\vec{S} = \vec{S}_2 - \vec{S}_1 \qquad 4\text{-}3$$

In equation (4-2), only partial information about $\vec{R}_1$ and $\vec{R}_2$ is available from measurements. Therefore, the equations implied by (4-2) actually differ in form for each combination of sensors considered, and will be set up and solved separately for each case. If the two sensor stations are part of a single flight over the area, $\vec{S}$, the relative position of station 2 with

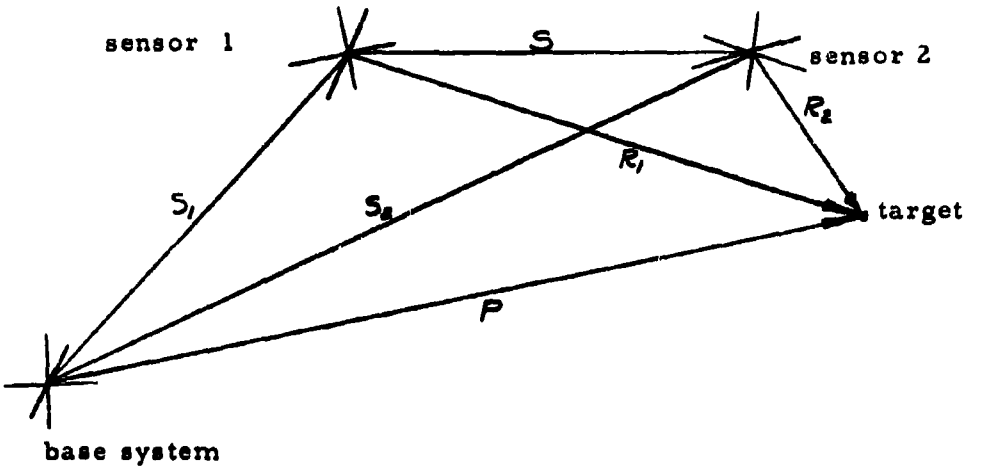

Figure 4.1 STEREO TARGET LOCATION

respect to 1, is in error only due to navigation from station 1 to 2. On the other hand, if the two sets of observations are made on separate flights, the navigation vectors S_1 and S_2 are measured, and $\vec{S}$ involves the errors in both vectors.

For the purposes of an error analysis, the complete solution to Equation 4-1 is not required. The error in $\vec{P}$ due to an error in a measurement of variable, ν, may be found by differentiation. If P_i is the i th component of vector $\vec{P}$ and ν_j is the j th measured variable ν, then:

$$(dP_i)_j = \frac{\partial P_i}{\partial \nu_j} d\nu_j \qquad 4\text{-}4$$

where $(dP_i)_j$ is the error in P_i due to the error in ν_j. The total error in P_i can be found from $(dP_i)_j$. Assuming that the ν_j's are chosen to be directly measured quantities, the errors in different ν_j's are independent. Statistically, if the $d\nu_j$ in Equation 4-4 is the probable error in ν_j, then the probable error in P_i due to all error sources is given by:

$$dP_i = \left[\sum_{j=1}^{J} (dP_i)_j^2\right]^{1/2} \qquad 4\text{-}5$$

If an over-all measure of target location accuracy is desired, the root mean square error in the magnitude of the distance between the actual target and its measured location may be calculated.* Consideration of vector error shows this to be simply:

$$dP = \left[\sum_{i=1}^{3} (dP_i)^2\right]^{1/2} \qquad 4\text{-}6$$

Combining Equations 4-4, 4-5 and 4-6:

$$dP = \left[\sum_{i=1}^{3}\sum_{j=1}^{J} \left(\frac{\partial P_i}{\partial \nu_j}\right)^2 \left(d\nu_j\right)^2\right]^{1/2} \qquad 4\text{-}7$$

Therefore, the required quantity is the $\left(\frac{\partial P_i}{\partial \nu_j}\right)$ matrix. The vector is given by Equation 4-1, which may be differentiated with respect to ν_j, component by component. This process yields:

* In some cases, the horizontal or vertical error in target location may be of interest. These separate errors may be calculated by changing Equation 4-6. All other parts of the analysis are applicable.

$$\frac{\partial P_i}{\partial w_j} = \frac{\partial (S_1)_i}{\partial w_j} + \frac{\partial (R_1)_i}{\partial w_j} \qquad 4\text{-}8$$

Since the components of S_1 are directly measured, $\frac{\partial (S_1)_i}{\partial w_j} = 0$ unless $w_j = (S_1)_i$, and $\frac{\partial (S_1)_i}{\partial (S_1)_i} = 1$. The matrix $\frac{\partial (R_1)_i}{\partial w_j}$ must be evaluated for each sensor combination, depending on the particular information about R_1 and R_2 which is measured by those sensors.

For the parametric study described later, three sensor combinations are used. These are: Panoramic camera stereo, side-looking radar stereo, and a panoramic camera combined with side-looking radar. The derivations of $\frac{\partial (R_1)_i}{\partial w_j}$ values for these cases are given in Appendices A, B, and C. Other possible sensor combinations would include Frame camera and IR. The long focal length cameras considered restrict frame cameras to narrow field angles. Over these angles, the geometry in frame and panoramic cameras are nearly identical, since the curved focal surface only affects larger angles. Therefore, the panoramic camera results at small angles may be assumed to be similar to what would be obtained for frame cameras. IR was not considered since the present state-of-the-art does not provide for high altitude capability. However, including IR results requires a straightforward extension of the calculations.

5. PARAMETRIC STUDY OF TARGET LOCATION ERRORS

5.1 General Description

The target location study was not to be tied to any particular state-of-the-art of any equipment involved, so the measurement errors were varied from presently expected values down to zero, to allow for future improvements. Tho altitude ranges considered are the regime of boost-glide type vehicles. The altitude range limits were 50,000 and 1,500,000 feet.(Thus including high altitude cruise type vehicles, as well as satellites.)

This parametric treatment of the problem has several purposes. Primarily, it is desired that the trade-offs between various combinations of sensors could be illustrated as a function of measurement errors and parameters such as sensor altitude. These comparisons and trade-offs are treated after the description of probable error calculations.

It is also possible to use the output of this study to predict the probable error in target location when any particular sensor combination is used. The error introduced by various measurement errors is provided as a function of geometrical factors (altitude, etc.) for each sensor combination.

From the target location error results, it is also possible to draw conclusions with respect to image restitution for purposes of image registration.

The parametric study described in the remainder of this section was carried out using the Laboratory's IBM 704 computer. The target location errors are computed by making use of the location error equations developed in the previous section and its appendices. The results are in the form of graphs for ease of examination. Two sets of graphs are presented; one which shows the contribution to target location error due to various measurement errors, as a function of location geometry, and a set which shows trade-offs between systems as a function of sensor measurement errors.

5.2 Error Contributions due to Various Sensor Errors

Three basic sensor combinations were chosen for the study. These are: Stereo Panoramic camera, Panoramic camera with side-looking radar, and Stereo radar. The frame camera, an obvious possible sensor choice, has not been included, since the geometry of frame and panoramic systems is sufficiently similar at small field angles that the error analysis is not affected by the choice. The panoramic camera was chosen rather than the frame camera in order to include larger field angles as well as the small angles of a frame system. Both front- and side-lap is considered for stereo measurements where applicable. (High resolution radar, at present, cannot be used for stereo by measuring with forward and rearward squinted antennas on a single flight line.)

Throughout the derivations of target location equations in Section 4 camera errors were assumed to be the errors in film measurement and focal length. It is clear that these are not the only sources of error. However, other errors can be included, since other errors can only affect the direction of the camera vector, just as film and focal length errors do. For example, atmospheric hydrostatic deflection effectively distorts the image, and is therefore equivalent to a film measurement error. Thus the errors in film and focal length measurement are sufficient to take into account all possible camera errors.

In order to reduce the number of separate error sources still further, so that the total output of information is not overwhelming, other error sources were grouped together. All navigation errors (error in $\vec{S}$, $\vec{S}_1$ and $\vec{S}_2$ of Section 4) were grouped and called simply navigation errors. Likewise, all roll, pitch and yaw errors which contribute to location error are included as stabilization errors. Film and focal length errors include those errors due to all cameras in the system. In the case of radar stereo, the antenna beam spread in the azimuthal direction adds directly to yaw errors in target location, so it is included as a stabilization error. The total number of groups of errors is therefore reduced to 5, namely:

1) Radar range error
2) Film measurement error
3) Focal length error

5-1

4) Navigation error

5) Stabilization error

These five errors can include all possible error sources in a system. Table 5.1 lists several examples.

The total target location error can be found from the error contributions by a simple procedure. Each curve plotted in Figures 5.3 to 5.20 shows the error contribution due to one of the 5 errors listed above. The error contribution is computed for unit error in each case, but for convenience in plotting, the values are then multiplied by constants, These constant multipliers are equivalent to assuming errors as:

1) Range measurement = $\pm$ 10 meters
2) Film measurement = $\pm$ 50 microns
3) Focal length measurement = $\pm$ 100 microns 5-2
4) Navigation component = $\pm$ 10 meters
5) Stabilization angles = $\pm$ 0.1 milliradians

If one wished to provide different estimates of these errors, he would compute total location error by reading the value of each error contribution from the appropriate graph, dividing by the constant listed in 5-2 to get the contribution from unit error, and multiplying by his estimate of error for that measurement. This yields the location error due to each error source. The total error is obtained by taking the square root of the sum of the squares of individual errors.

Defining:

$dR, dX, dF, dN, dSTAB$ = errors 1 to 5 listed in 5-1, measured in units given with values in 5-2.

C_1, C_2, C_3, C_4, C_5 = error contributions due to errors 1 to 5, the values being read from the graphs.

Then, the target location error is given (assuming normal distribution of errors) by:

$$\text{Error (in meters)} = \left\{\left[\frac{C_1 dR}{10}\right]^2 + \left[\frac{C_2 dX}{50}\right]^2 + \left[\frac{C_3 dF}{100}\right]^2 + \left[\frac{C_4 dN}{10}\right]^2 + \left[\frac{C_5 dSTAB}{0.1}\right]^2\right\}^{1/2} \quad 5\text{-}3$$

Table 5.1 TYPICAL ERROR SOURCES

1. Radar Range Error
    1. Timing error
    2. Finite pulse length effect
    3. Processing errors

Camera Errors

2. Film Measurement - errors which vary over the format
    1. Film measurement
    2. Nonuniform film shrinkage
    3. Lens distortion
    4. Atmospheric distortion
        hydrostatic gradient
        refraction at shock wave, boundary layer and intermediate region
    5. Window distortion
    6. Variations of scan angle such as caused by off-center mounting of scanning prism and other mechanical errors.
    7. Improper film flattening

3. Focal Length - errors in scale which do not vary over the format, but may vary from picture to picture
    1. Focal length determination
        calibration
        tolerances in camera
        expansion caused by temperature changes
    2. Uniform film shrinkage

4. Navigation
    1. Errors in inertial system
    2. Errors in marking of film or tape
    3. Errors in control point locations

5. Stabilization
    1. Errors in stabilizing mount
    2. Errors in marking
    3. Radar synthetic antenna beam width

An example of this process is given in Figures 5. 1 and 5. 2.

The error contributions are plotted as functions of five parameters. These are: the altitude of sensor 1 (H_1), the altitude of sensor 2 (H_2), the field angle or angle from the vertical to the line between sensor 1 and the target (A), the camera focal length (F), and the side offset of sensor 2 with respect to sensor station 1 (S_y). The last parameter (S_y) is used only as zero or nonzero to separate forward and side-lap location.

It is obviously useless to plot all combinations of the five parameter values. Instead, a single set of values was picked as a starting point, and all parameters were varied separately, holding the others at the chosen values. The chosen set of values used as a basis is:

$$\begin{aligned} H_1 &= 100 \text{ Kft} \\ H_2 &= 100 \text{ Kft} \\ A &= 30° \\ F &= 1 \text{ m} \\ S_y &= 0 \text{ or } \neq 0, \text{ plotted separately} \end{aligned} \qquad 5\text{-}4$$

The parameters are varied through the following ranges, as suggested by the sponsoring agency:

$$\begin{aligned} H_1, H_2 &= \begin{cases} 50 - 1500 \text{ Kft for cameras} \\ 50 - 100 \text{ Kft for radar} \end{cases} \\ A &= 0 - 60 \text{ degrees from vertical} \\ F &= 0.15 - 2 \text{ meters} \end{aligned} \qquad 5\text{-}5$$

The maximum allowable baseline for forward-lap photography was set by a choice of a 9-inch-wide format, which limits the target angle ahead or behind the camera which still appears on the film. The side-looking radar was assumed to have the antenna beam set at right angles to the flight direction. No restriction is set on the field angle at which the radar can operate, but it must be realized that at very small angles the resolution will not be sufficient to identify a target. As discussed previously, it has been assumed throughout the target location analysis that the target is identifiable on each sensor record.

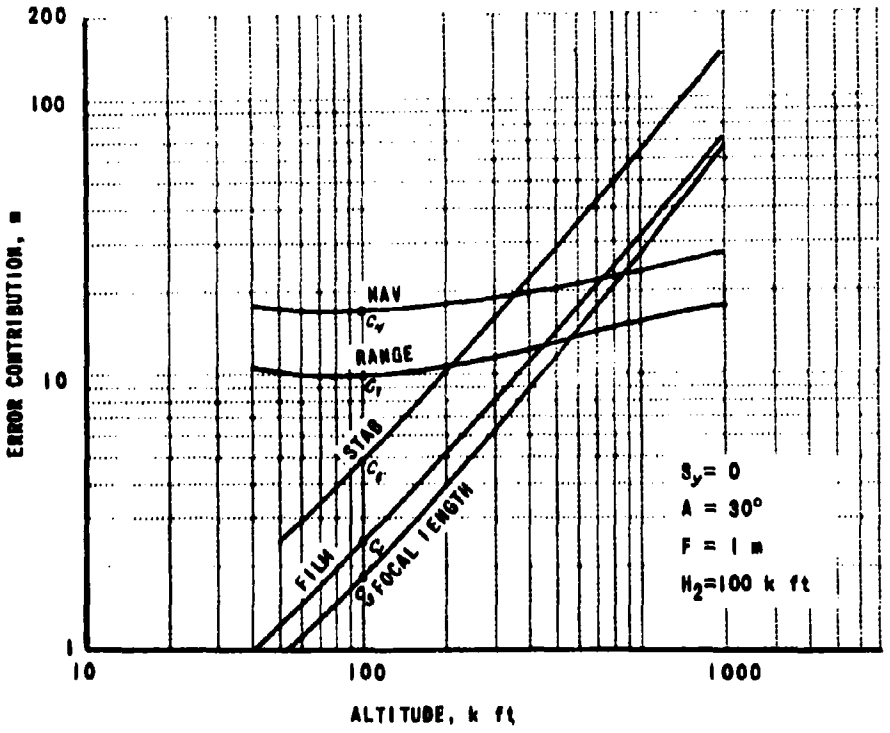

Figure 5.1 PAN-RAD SYSTEM - VARIATION WITH ALTITUDE OF SENSOR ONE

Total Location Error Calculation

Assume: $H_1 = H_2 = 100$ Kft

$A = 30°$

$F = 1$ m.

$S_y = 0$

$dR = 3$ m.

$dX = 10$

$dF = 100$

$dN = 30$ m.

$dSTAB = 0.1$ milliradian

From graph $C_1 = 10.051$ m.

$C_2 = 2.489$

$C_3 = 1.877$

$C_4 = 17.380$

$C_5 = 5.016$

From Equation 5-3:

$$\text{Error} = \left\{ \left[\frac{(10.051)(3)}{10} \right]^2 + \left[\frac{(2.489)(10)}{50} \right]^2 + \left[\frac{(1.877)(100)}{100} \right]^2 + \left[\frac{(17.380)(30)}{10} \right]^2 + \left[\frac{(5.016)(0.1)}{0.1} \right]^2 \right\}^{1/2}$$

Error = 53 m

Figure 5.2 EXAMPLE OF ERROR CALCULATION

5.3 Error Contribution Results

5.3.1 Panoramic Camera Stereo ("Twopan")

Considering the forward-lap photographs first, it can be seen that as the altitude of the cameras is increased, the error due to anything except navigation is proportional to altitude, while navigation error is altitude independent, Figure 5.3. Varying field angle has very slight effect on error, with a slight increase in location errors at larger angles, Figure 5.4.

Varying the focal length, Figure 5.5, has several effects. A shorter focal length means smaller scale, and correspondingly allows a longer base line(separation of the two camera stations)for triangulation. Therefore, navigation and stabilization errors have less effect on short focal length systems. A fixed error in focal length, of course, produces a greater percent change at short focal length, thus contributing more to location error. The effects of scale change and base line change effectively balance for film errors, causing film error contribution to be almost independent of focal length.

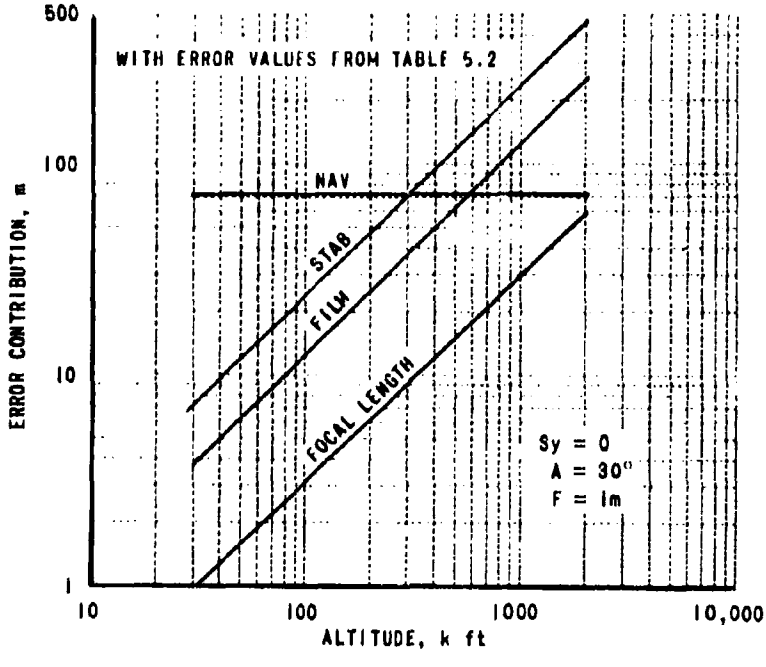

Figure 5.3 TWO-PAN SYSTEM - VARIATION WITH ALTITUDE

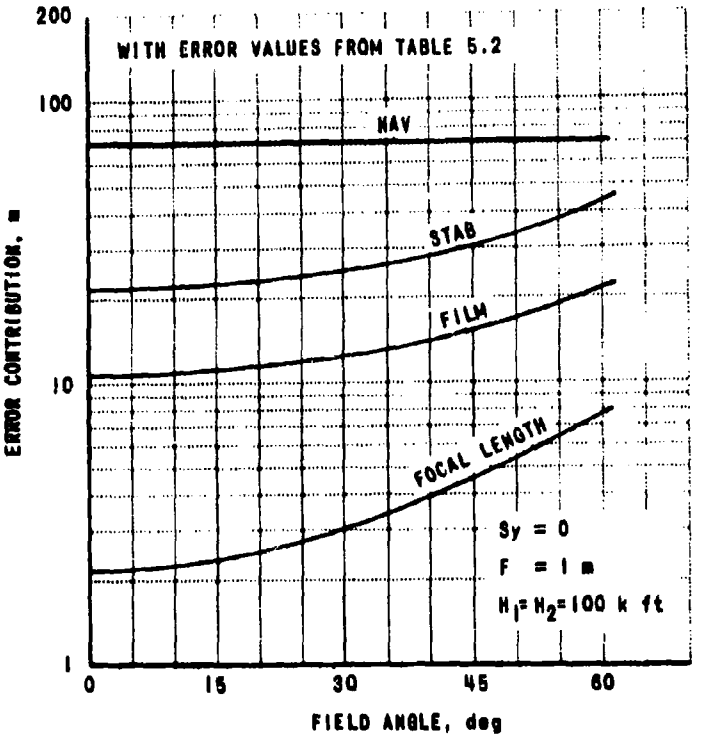

Figure 5.4 TWO-PAN SYSTEM - VARIATION WITH FIELD ANGLE

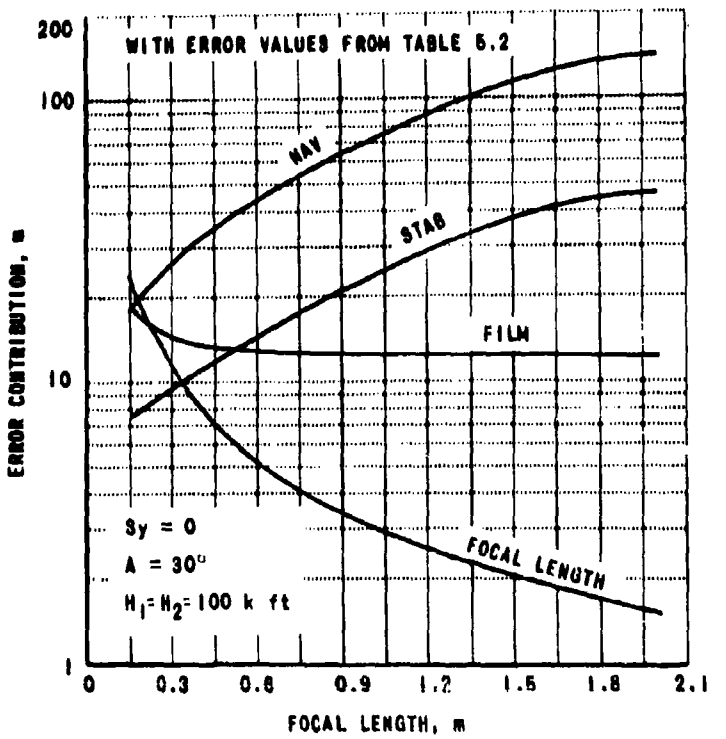

Figure 5.5 TWO-PAN SYSTEM - VARIATION WITH FOCAL LENGTH

The case of side-lap stereo is similar to forward-lap. Because of slightly different geometry, the curves are not identical, but the same general character is shown, Figures 5.6 and 5.7. In the case of variation of focal length, the base line for side-lap, Figure 5.8, was kept fixed, so that the curves for contribution due to navigation and stabilization become almost independent of focal length, while film error contribution follows the same form as focal length contribution, due to scale change.

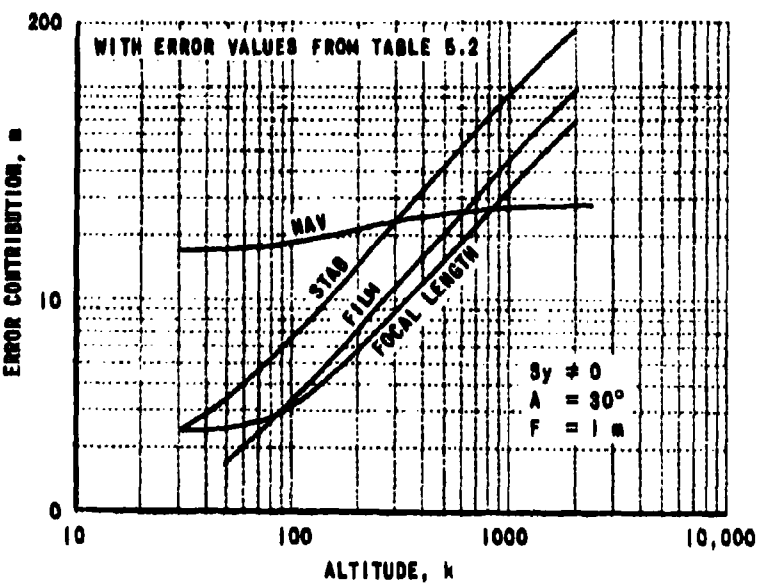

Figure 5.6 TWO-PAN SYSTEM VARIATION WITH ALTITUDE

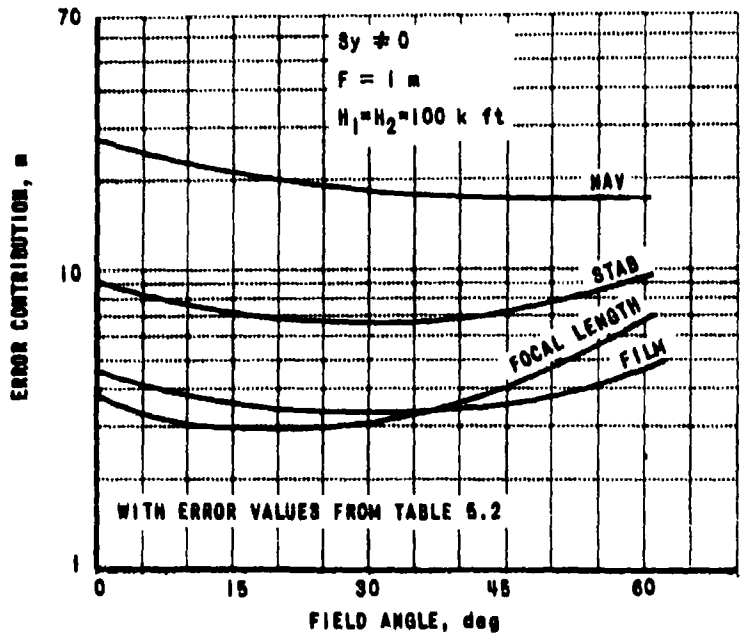

Figure 5.7 TWO-PAN SYSTEM - VARIATION WITH FIELD ANGLE

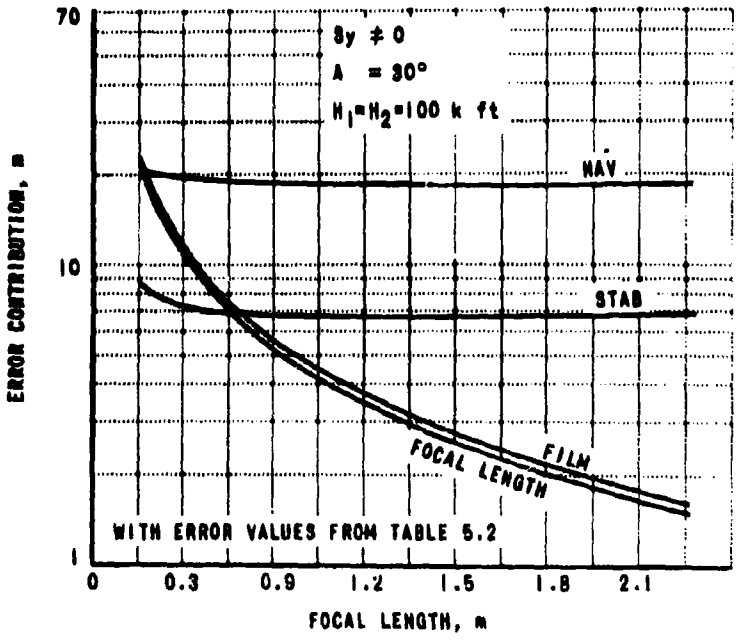

Figure 5.8 TWO-PAN SYSTEM - VARIATION WITH FOCAL LENGTH

5.3.2 Panoramic Camera with Radar ("Panrad")

A system combining a camera with radar makes use of the direction determination by the camera and the range determination of the radar. If the photograph is taken from nearly the same place as the radar record, the combination provides range from the radar and angles from the camera to fix a single vector. If the two sensors are used far apart, the situation is more complicated. The target location error becomes extremely large if the lines from the target to each sensor meet at right angles, since the location is then found as the intersection of a sphere and a tangent line. Thus, for certain base lines, the system fails, just as photographic stereo fails if the base line is reduced toward zero.

As in the photographic stereo system, then, the two sensor stations can be either essentially on the same flight path ($S_y \approx 0$) or on separated paths ($S_y \neq 0$). As previously discussed, the radar sensor altitude was held at 100 Kft or less. This means that the cases listed as $S_y \approx 0$ are situations where the camera and radar sensors are carried either at the same altitude (possibly 1 vehicle) or else that the two flights are at different altitudes, but are close enough to each other horizontally that the target is on the same side of both flight lines.

Examining Figure 5.9, it can be seen that for $S_y \approx 0$ the error contributions as a function of camera altitude are much like those for two camera stereo, with the addition that radar range error contribution is essentially independent of camera altitude. Figure 5.10 shows that target location error is independent of radar sensor altitude over a factor of two in altitude.

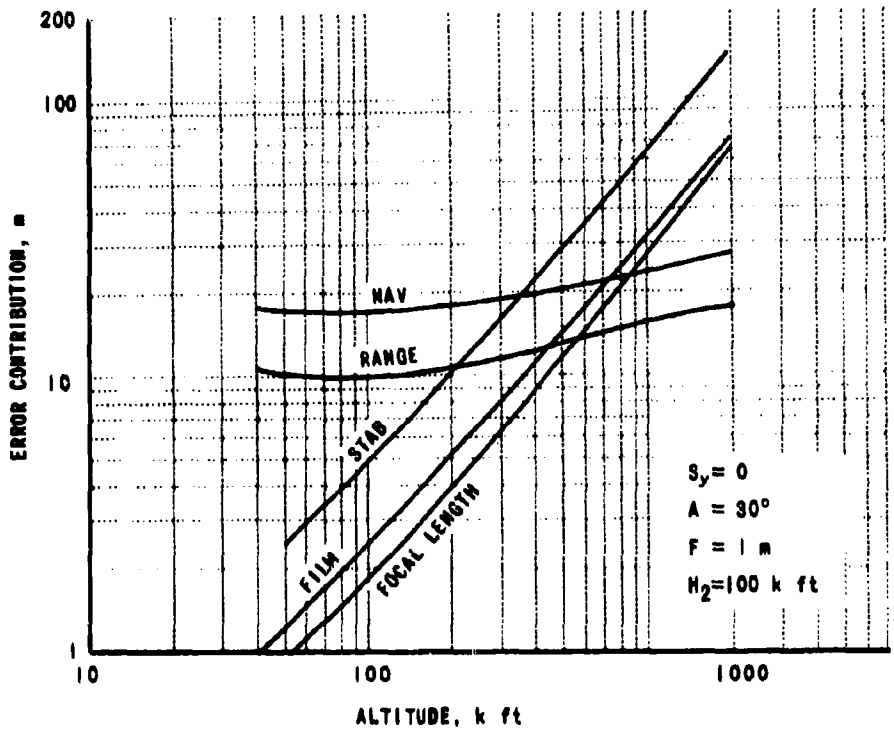

Figure 5.9 PAN-RAD SYSTEM - VARIATION WITH ALTITUDE OF SENSOR ONE

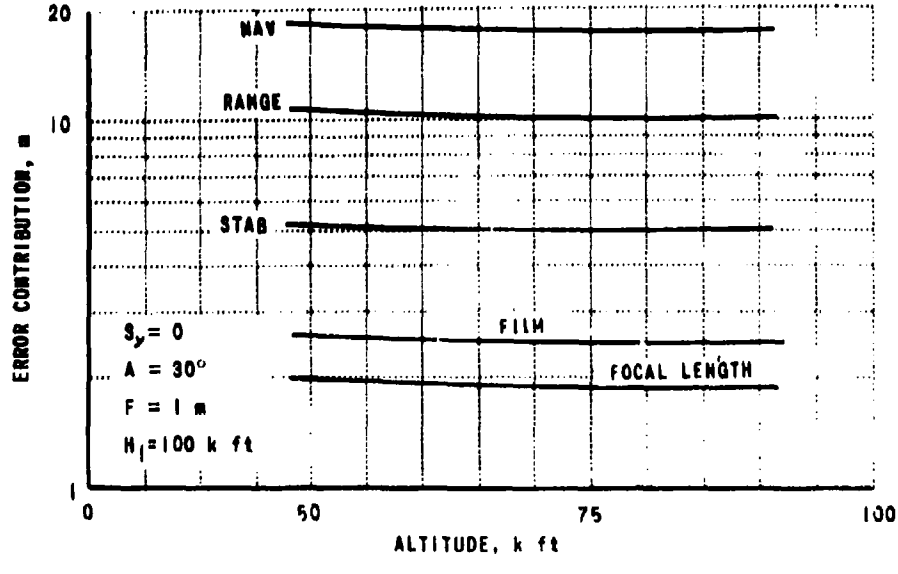

Figure 5.10 PAN-RAD SYSTEM - VARIATION WITH ALTITUDE OF SENSOR TWO

As with 2 cameras, a camera combined with a radar on nearly the same flight path ($S_y \cdot 0$) yields target location errors which are nearly independent of field angle. It is apparent from Figure 5.11, however, that the contribution to location error due to focal length error increases with field angle, becoming more critical at larger angles.

The system requirements for camera error limits become less severe as the photographic scale is increased. This can be seen in Figure 5.12 showing error contribution as a function of focal length of the camera. As focal length is increased, the scale becomes larger, and the location error due to camera measurements becomes less.

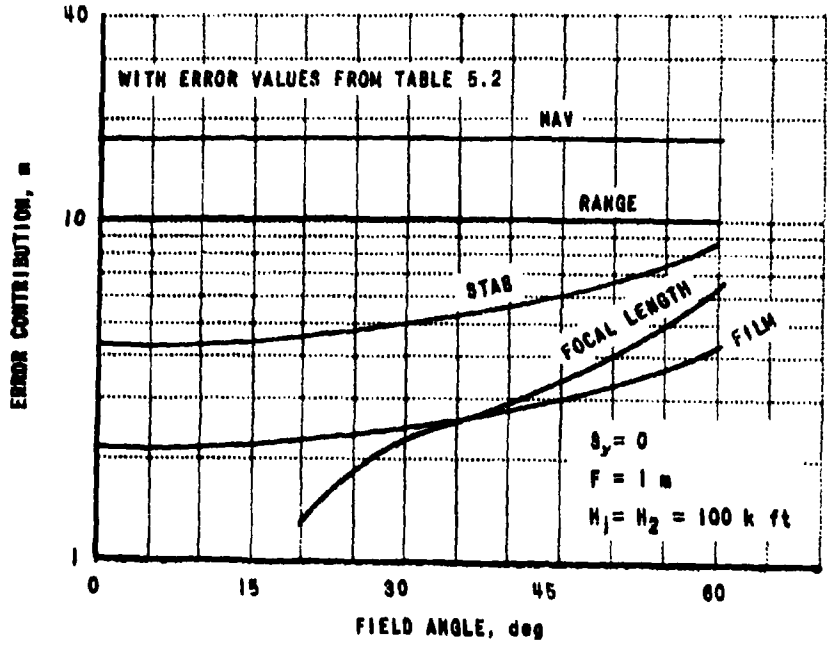

Figure 5.11 PAN-RAD SYSTEM - VARIATION WITH FIELD ANGLE

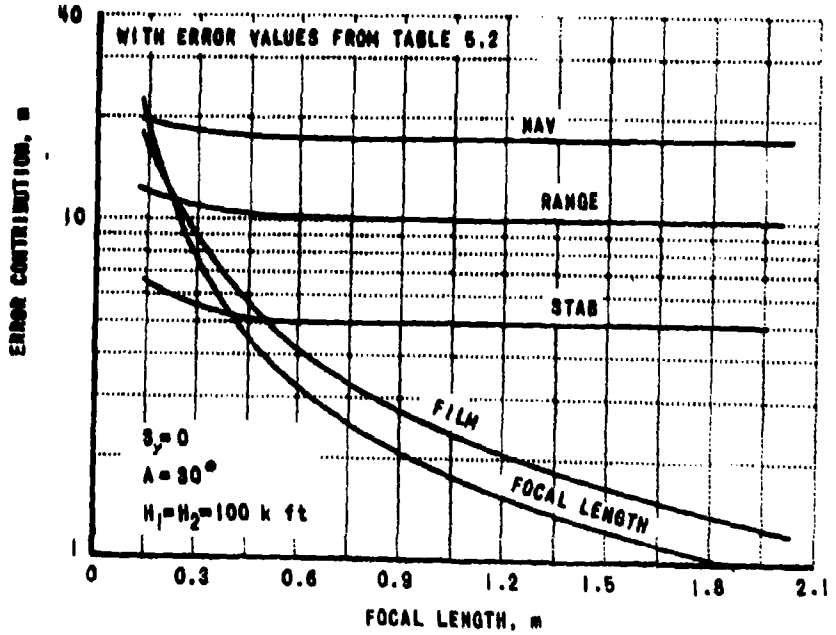

Figure 5.12 PAN-RAD SYSTEM - VARIATION WITH FOCAL LENGTH

If the camera and radar are carried on separate flights which pass opposite sides of the target ($S_y \neq 0$), the poor location geometry that may occur can cause large errors.

As camera altitude is varied, Figure 5.13, the same general trends occur as with $S_y = 0$, but the poorer geometry causes over-all larger error contributions. Varying the radar altitude, keeping the target location with respect to the camera fixed, Figure 5.14, causes the two position vectors to intersect at 90° when the radar is at about 76 Kft. Thus the error becomes extremely large at that point.

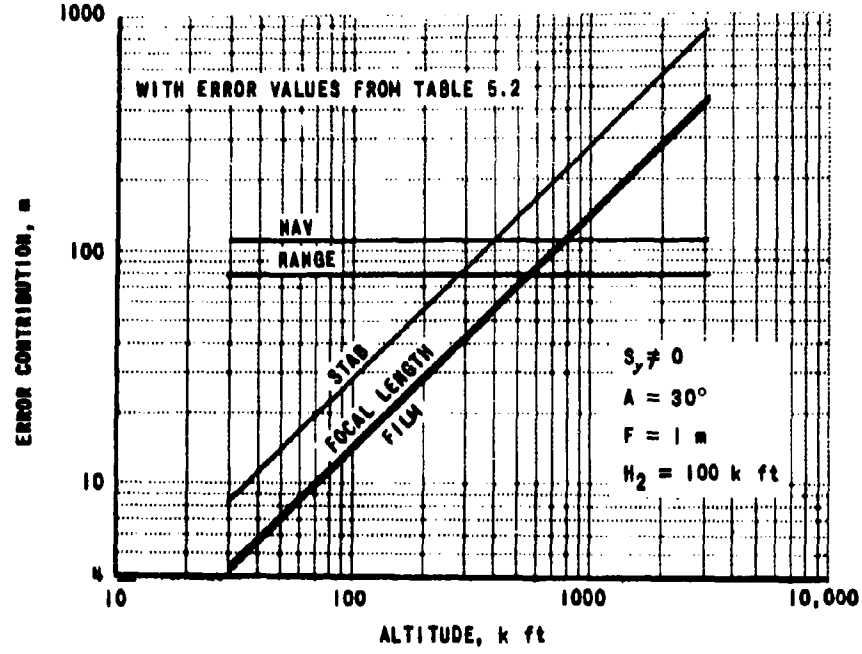

Figure 5.13 PAN-RAD SYSTEM - VARIATION WITH ALTITUDE OF SENSOR ONE

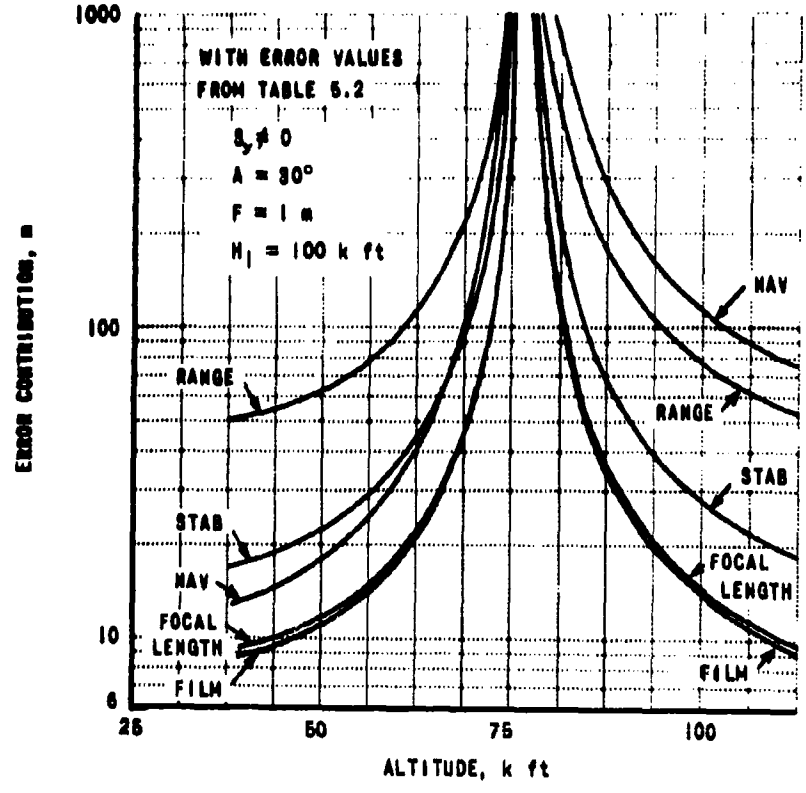

Figure 5.14 PAN-RAD SYSTEM - VARIATION WITH ALTITUDE OF SENSOR TWO

Similarly, as the field angle is varied, Figure 5.15, the critical geometry is reached at about 37°, again causing extremely large errors. This corresponds to the poor geometric situation which arises when two photographs to be used for stereo are taken from nearly the same point.

Regardless of geometry, error contributions due to radar range, camera stabilization and navigation errors are independent of scale, and camera errors contribute less as the scale is increased by increasing focal length, Figure 5.16.

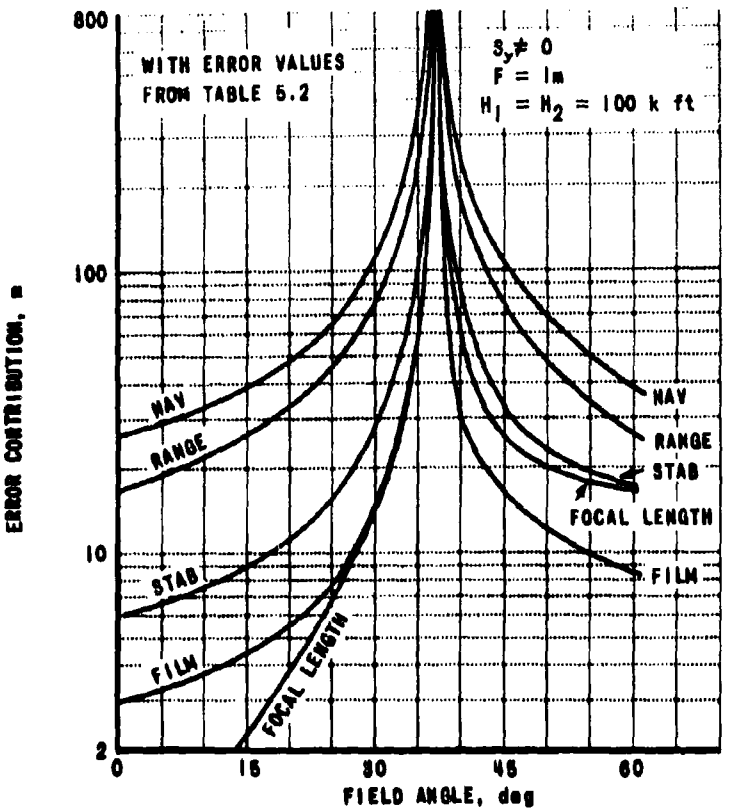

Figure 5.15 PAN-RAD SYSTEM - VARIATION WITH FIELD ANGLE

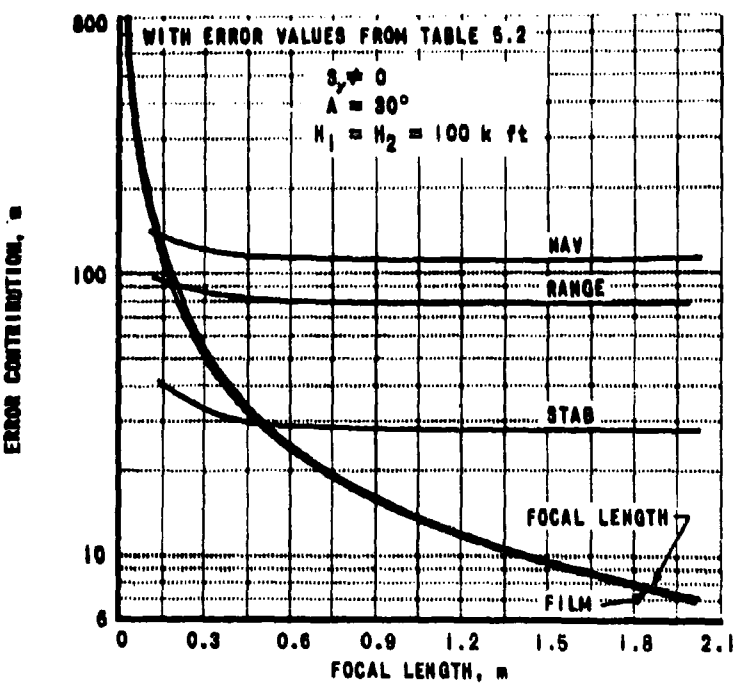

Figure 5.16 PAN-RAD SYSTEM - VARIATION WITH FOCAL LENGTH

5.3.3 Radar Stereo ("Tworad")

Radar stereo relies upon a knowledge of two ranges to locate a target on a circle; the target is then located since it must be within the radar antenna beam as well as on the circle. The two radar sensor stations must be on separate flights since the side-looking radar records the target image at essentially 90° to the flight line.

Figure 5.17 shows error contributions as a function of sensor altitude, when the two sensor stations are separated horizontally (parallel flights). The only variation observed is that due to stabilization. That error becomes more critical at higher altitude only because the target field angle was kept fixed, so the target was farther away horizontally when the sensor was higher. Since the radar antenna beam is used to help locate the target, a yaw error becomes more critical for greater horizontal distance to the target.

Figure 5.18 shows a similar effect for stabilization error as the horizontal distance is increased by increasing field angle. Since side-looking radar will not work at small angles from vertical, the navigation and range error contributions become large at small angles.

If an attempt is made to use two radars at different altitudes, but nearly the same horizontal position, location errors increase as vertical separation decreases, as shown in Figure 5.19.

Table 5.2 NOMINAL ERROR VALUES

1) Range measurement = $\pm$ 10 meters
2) Film measurement = $\pm$ 50 microns
3) Focal length measurement = $\pm$ 100 microns
4) Navigation component = $\pm$ 10 meters
5) Stabilization angles = $\pm$ 0.1 milliradians

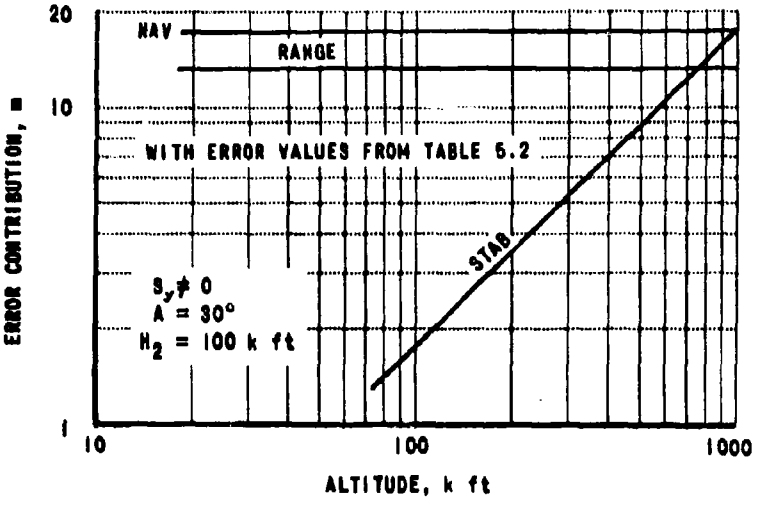

Figure 5.17 TWO-RAD SYSTEM - VARIATION WITH ALTITUDE OF SENSOR ONE

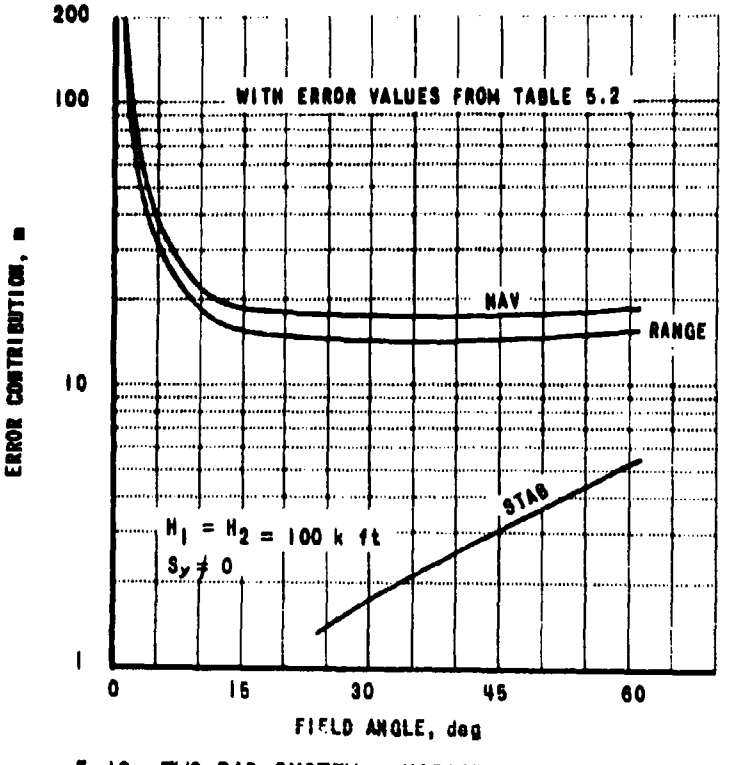

Figure 5.18 TWO-RAD SYSTEM - VARIATION WITH FIELD ANGLE

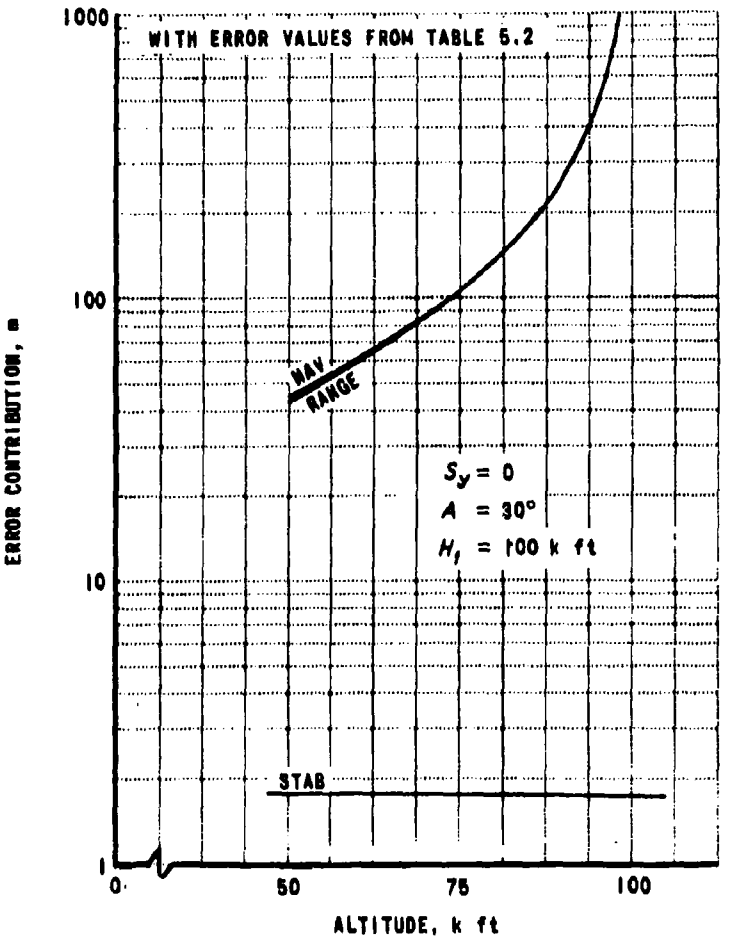

Figure 5.19 TWO-RAD SYSTEM - VARIATION WITH ALTITUDE OF SENSOR TWO

5.4 Comparisons of Different Sensor Combinations

In the previous section, the results of the parametric study were presented. However, the form in which the results are presented does not lend itself to easy comparisons of different system capabilities. Therefore, a few representative situations were chosen, and the total target location error was plotted as a function of various system errors, allowing trade-offs between sensor combinations to be shown directly.

The sample cases picked were: high and low altitude cameras used for forward and side-lap stereo, and corresponding cases for the other two sensor combinations used. Again, radar is limited to operate at 100 Kft or less. Four cases are plotted for each sensor combination. The parameter values are given in Table 5.3.

In order to further reduce the large number of cross-plots, system errors were combined in two more cases. First, since the only stabilization error which enters for radar stereo is yaw error, and since even using coherent radar the effective antenna beamwidth is the order of a milliradian or more, the combined error due to yaw and antenna beam spread was held constant at 1 milliradian for the study.

Second, to obtain a single number for camera error, define:

$a_x\, dX_f$ = error contribution due to error (dX_f) in film measurement

$a_f\, dF$ = error contribution due to error (dF) in focal length measurement

Since these errors are independent, they should be added as root mean square values. The result is:

$$R.E. = \left[a_x^2 dX_f^2 + a_f^2 dF^2\right]^{1/2} \qquad 5\text{-}6$$

But the last equation may be rewritten:

$$R.E. = a_f dF \left[1 + \left(\frac{a_x}{a_f}\right)^2 \left(\frac{dX_f}{dF}\right)^2\right]^{1/2} \qquad 5\text{-}7$$

Table 5.3 PARAMETER VALUES FOR CHOSEN CASES

	2 Panoramic Cameras		Panoramic Camera with Radar			2 Radars		All Systems	
Case	Altitude of cameras	Focal length	Camera Alt.	Camera Focal length	Radar Alt.	Radar 1 Alt.	Radar 2 Alt.	Target Position	Side-Lap
I	100 Kft	1 m.	100 Kft	1 m.	100 Kft	100 Kft	100 Kft	30°	Yes
II	100	1 m.	100	1 m.	100 Kft	100 Kft	50	30°	No
III	1000	1 m.	1000	1 m.	100 Kft	100 Kft	100	30°	Yes
IV	1000	1 m.	1000	1 m.	100 Kft	100 Kft	50	30°	No

Since film measurement error is usually small compared to focal length error, the term in brackets is not much different from unity in many cases. Camera error is defined as:

$$C.E. = \frac{R.E.}{a_F} \cdot \left[1 + \left(\frac{a_x}{a_F}\right)^2 \left(\frac{dx_F}{dF}\right)^2\right]^{1/2} dF \qquad 5\text{-}8$$

Each graph is plotted showing target location error versus camera error (as just defined) for each system, with radar error as a parameter. Separate graphs show cases I to IV and different navigation and stabilization errors. Errors were chosen in the ranges:

$$\begin{aligned} &\text{Camera error - 0 to 1000 } \mu \\ &\text{Radar error - } \begin{cases} \text{1 to 10 meter range error} \\ \text{1 milliradian beamwidth} \end{cases} \\ &\text{Navigation error - 1 to 30 meters} \\ &\text{Stabilization error - .01 to .1 milliradian} \end{aligned} \qquad 5\text{-}9$$

Navigation errors can well exceed 30 meters, of course, but the results show that larger errors than this will override the effects of all other errors. This can also be seen by referring to any of the graphs in subsection 5.3 where a navigation error of 10 meters is seen to contribute errors which are larger than or at least comparable to any other error source.

5.5 Results of System Comparisons

The results of the system comparison study are presented graphically at the end of this section. The desirable system to be used for target location is that system which produces the smallest target location error, that is, the system which is represented by the lowest curve on a figure. Frequently two curves cross, in which case the better system is the one for which the location error curve is lower at the value of camera error which is attainable.

Using Figure 5.20 as an example, it can be seen that stereo panoramic cameras (2 Pan) are the best location system as long as camera error is less than 720 microns. If camera error is greater than that value (probably due to focal length errors), radar stereo (2 Rad) would be better, if range error can be held to 1 meter. The camera-radar (Panrad) combination is preferred over 2 Rad only when camera error is less than 80 microns with radar range error of 1 meter.

Figures 5.21 to 5.23 show low altitude (100 Kft), separated, parallel flights over a target (Case I, Section 5.4). Comparison of 5.20 and 5.21 show that stabilization error does not appreciably affect results at these attitudes if held under 0.1 milliradian, which should be possible. Figures 5.21 to 5.23 illustrate the effect of increasing navigation error.

It is clear that Panrad is not to be used for this situation, and that photography is better than radar so long as camera error is less than about 700 microns. If navigation errors become larger than about 10 meters, radar and photographic stereo yield comparable results.

It should be noted that navigation and stabilization errors need not be as large as would be the case for self-contained systems. The errors may be reduced by using control extension techniques, and/or ground based tracking systems. These reduced navigation errors can be used with the graphs presented here, to evaluate any target location system.

Figures 5.24 to 5.27 show the location errors when one flight line is used (or one flight above another for radar). It can be seen in general that this geometry is ideal for a panoramic-radar combination and that this system should outperform even a 2 photo determination, provided that equivalent navigational and orientation data are available. The photographic stereo will only produce better results if camera error is very small and navigation data is excellent. If navigation errors exceed 10 meters, radar becomes preferable to photographic stereo, since radar target location is less affected by navigation errors.

The cases in which the cameras are carried at high altitude (1,000 Kft) are shown in Figures 5.28 to 5.37.

The discussion of the low altitude cases can be applied as well to high altitudes, except that given navigation and stabilization errors introduce larger target location errors than at lower altitudes.

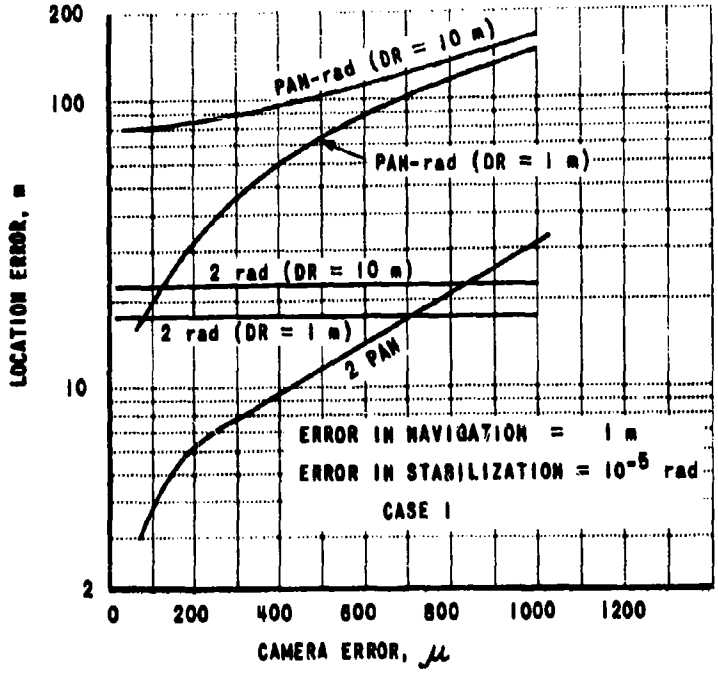

Figure 5.20 TARGET LOCATION ERROR

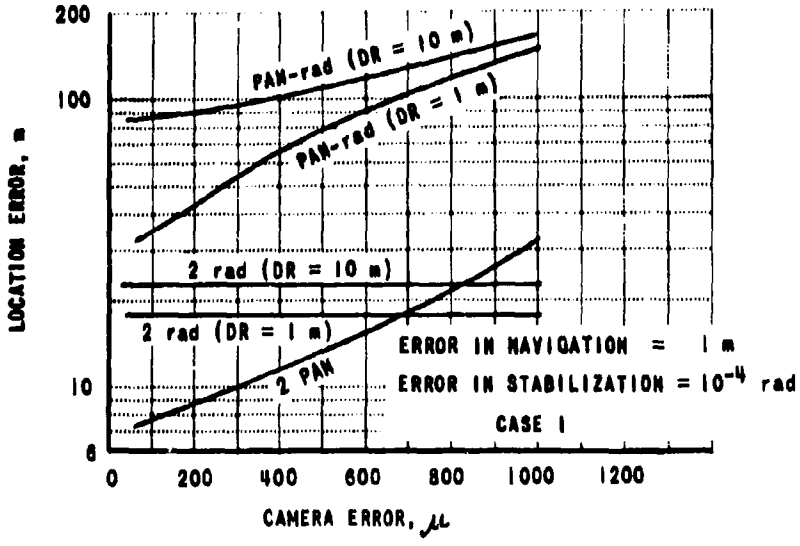

Figure 5.21 TARGET LOCATION ERROR

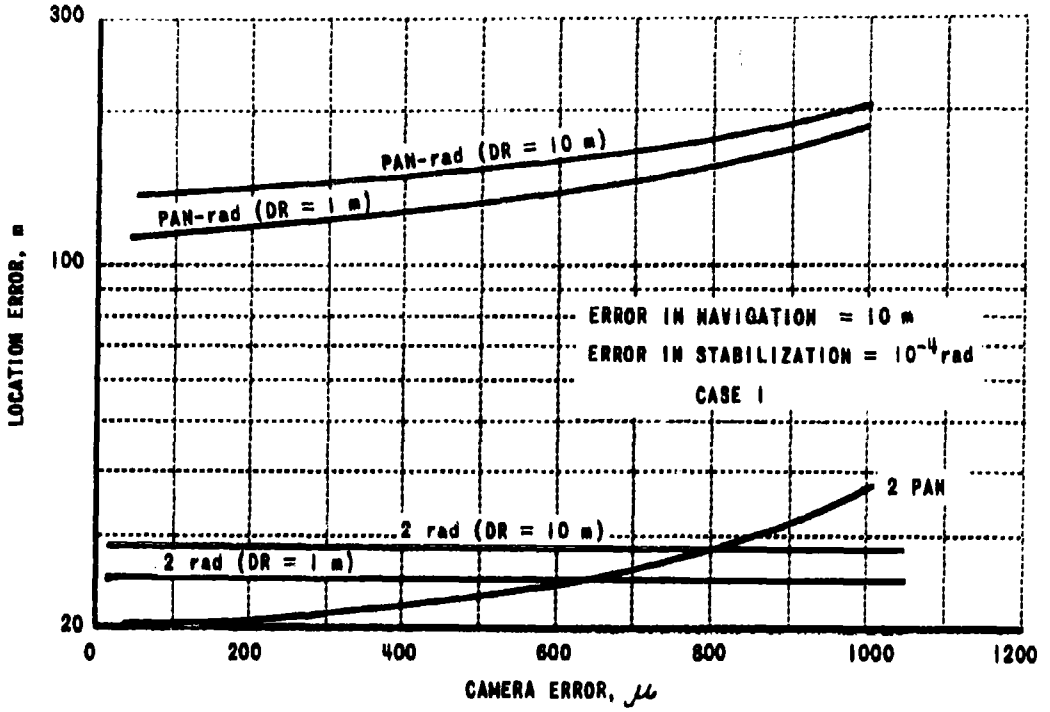

Figure 5.22 TARGET LOCATION ERROR

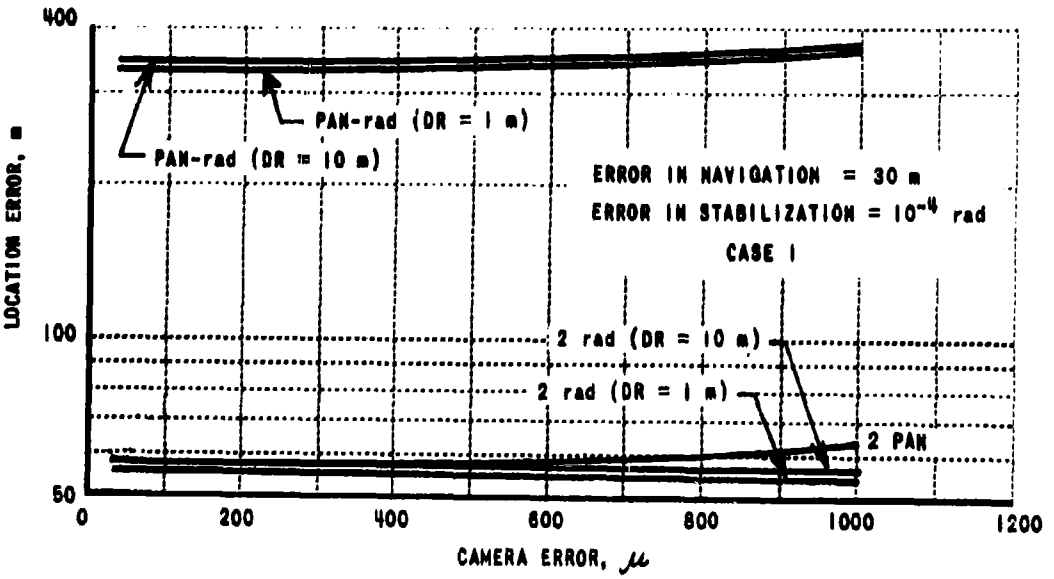

Figure 5.23 TARGET LOCATION ERROR

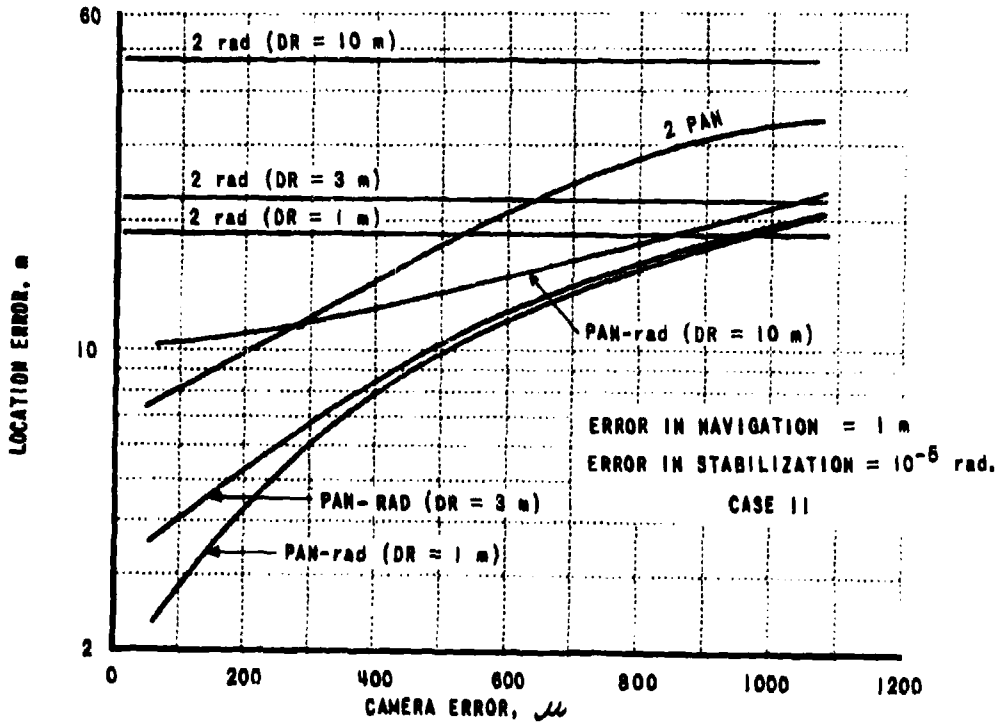

Figure 5.24 TARGET LOCATION ERROR

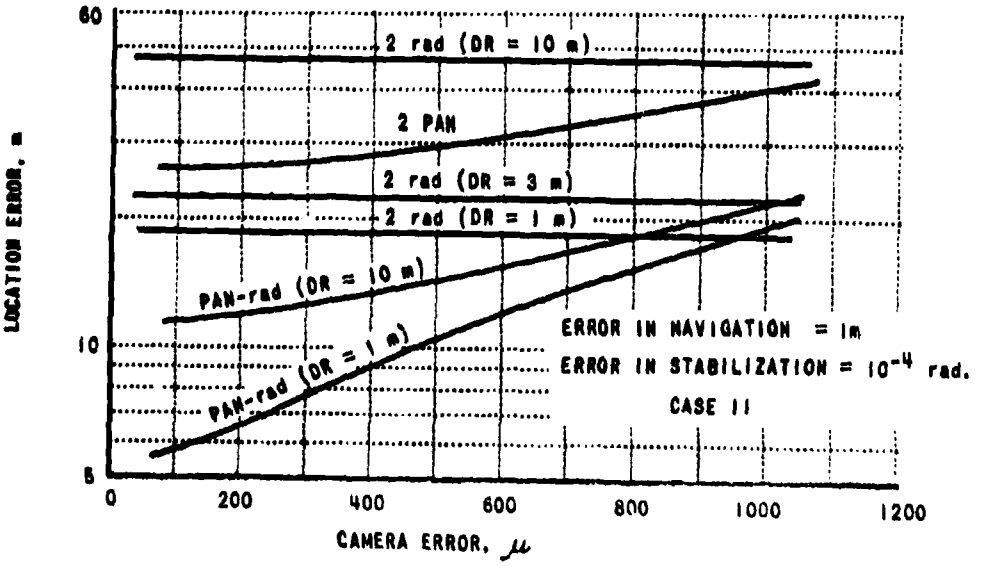

Figure 5.25 TARGET LOCATION ERROR

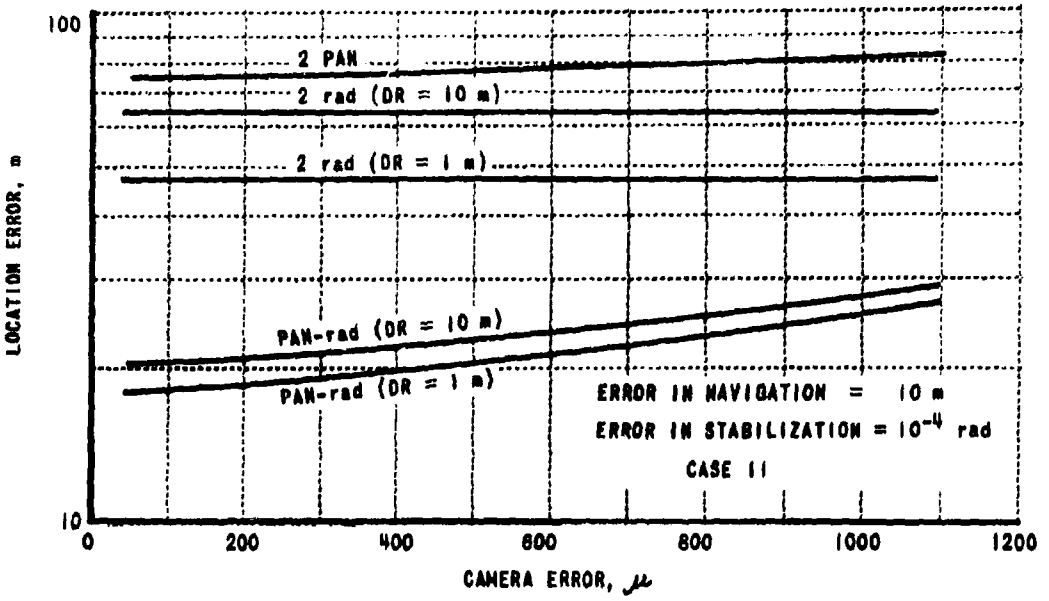

Figure 5.26 TARGET LOCATION ERROR

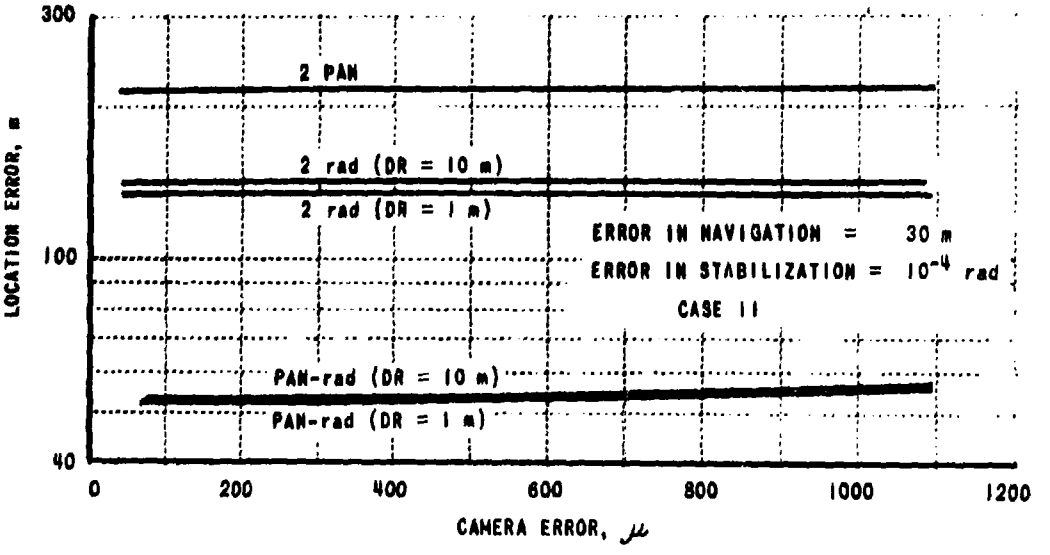

Figure 5.27 TARGET LOCATION ERROR

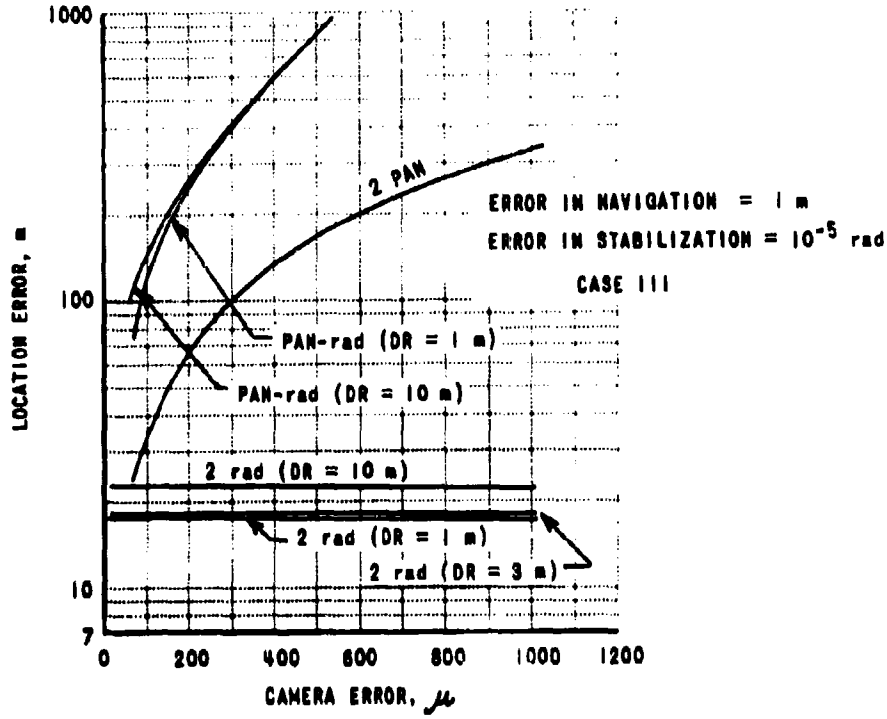

Figure 5.28 TARGET LOCATION ERROR

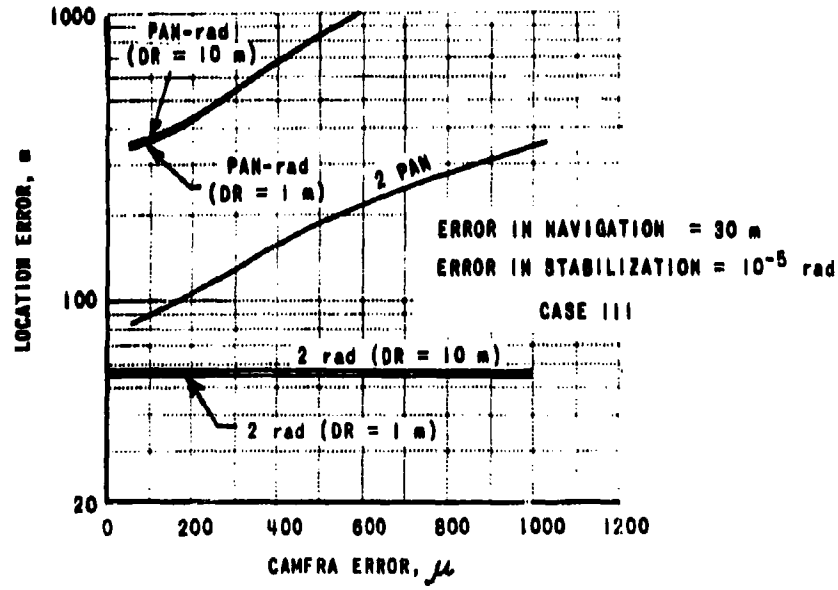

Figure 5.29 TARGET LOCATION ERROR

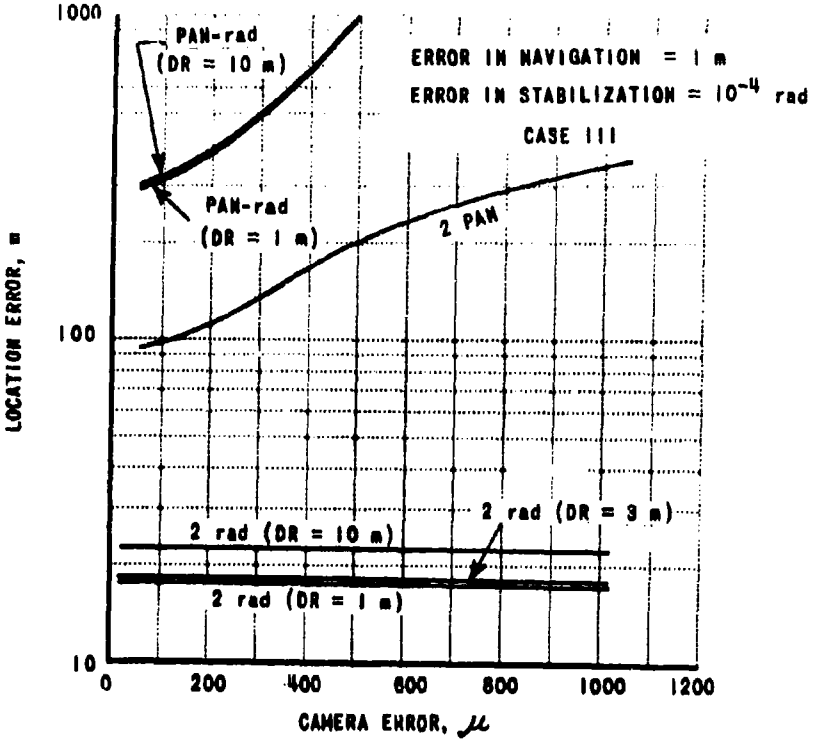

Figure 5.30 TARGET LOCATION ERROR

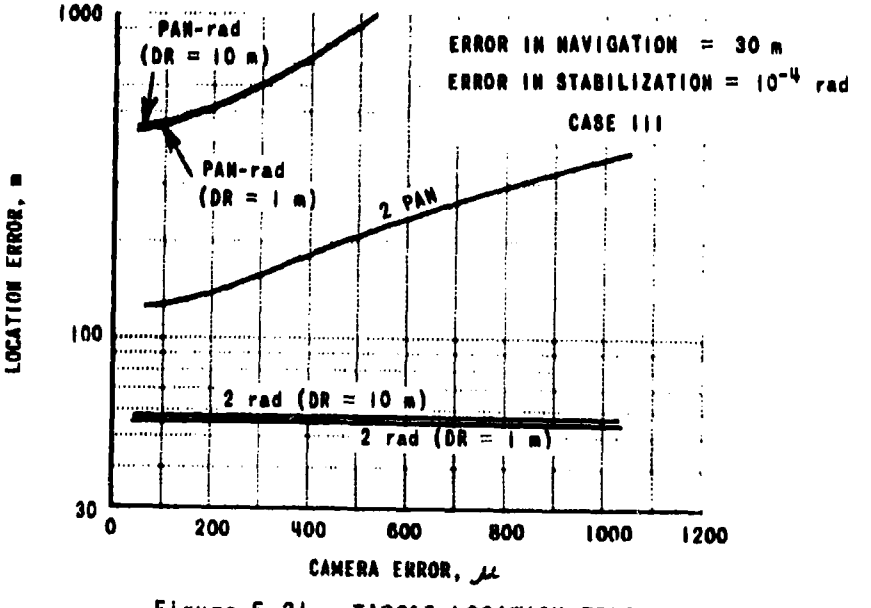

Figure 5.31 TARGET LOCATION ERROR

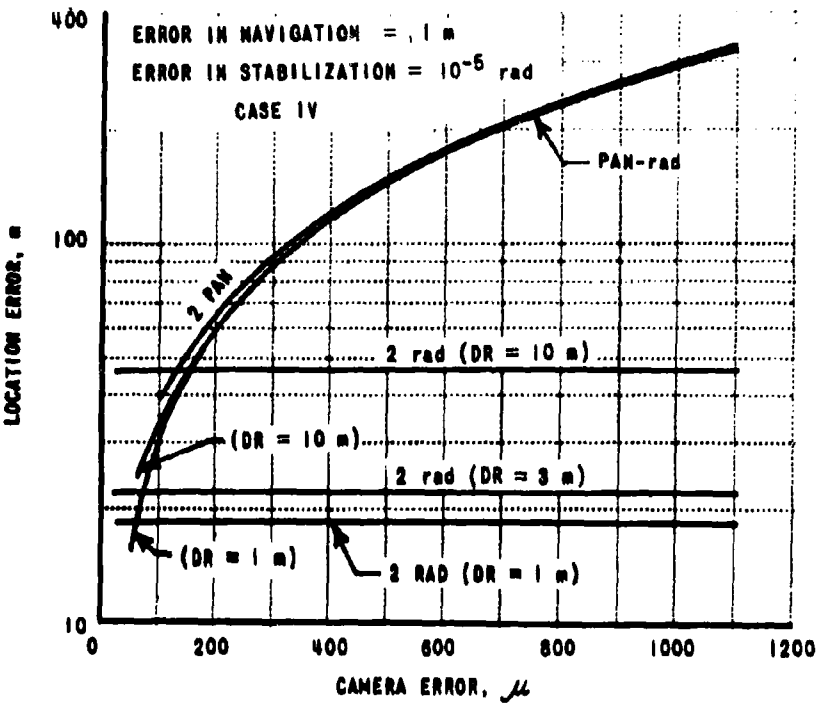

Figure 5.32 TARGET LOCATION ERROR

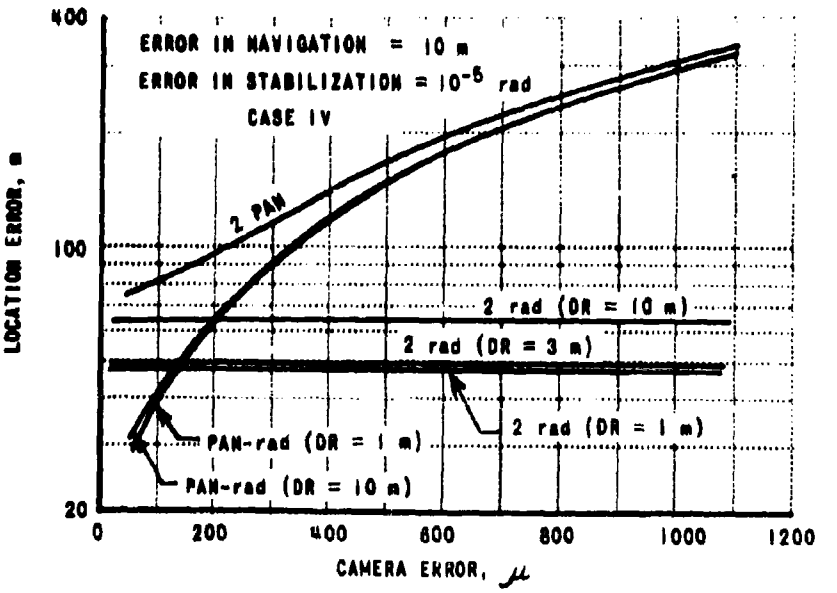

Figure 5.33 TARGET LOCATION ERROR

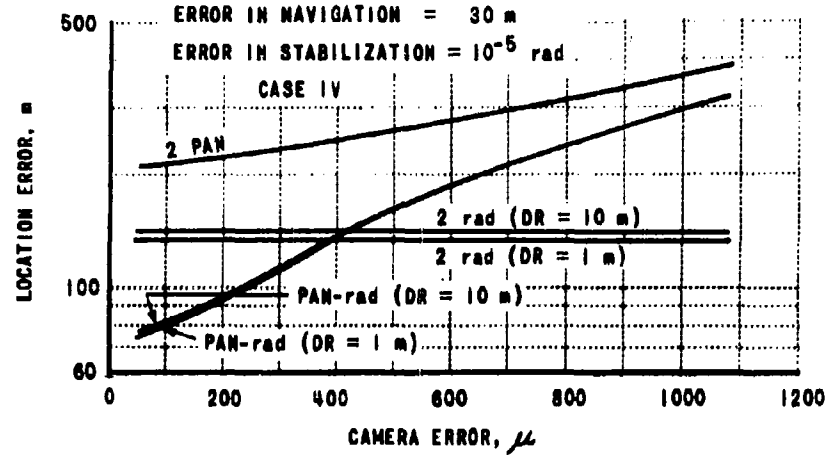

Figure 5.34 TARGET LOCATION ERROR

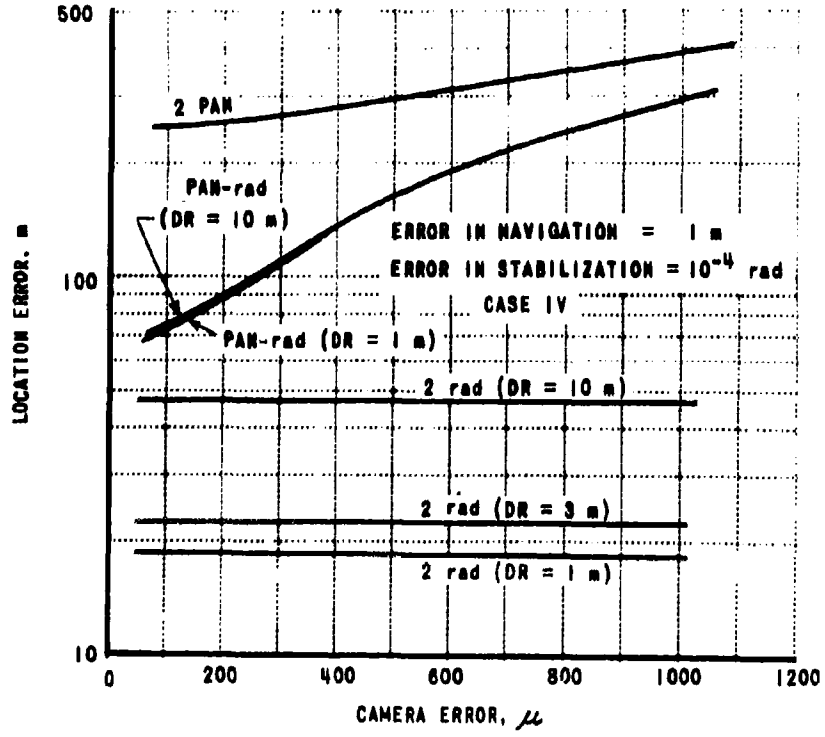

Figure 5.35 TARGET LOCATION ERROR

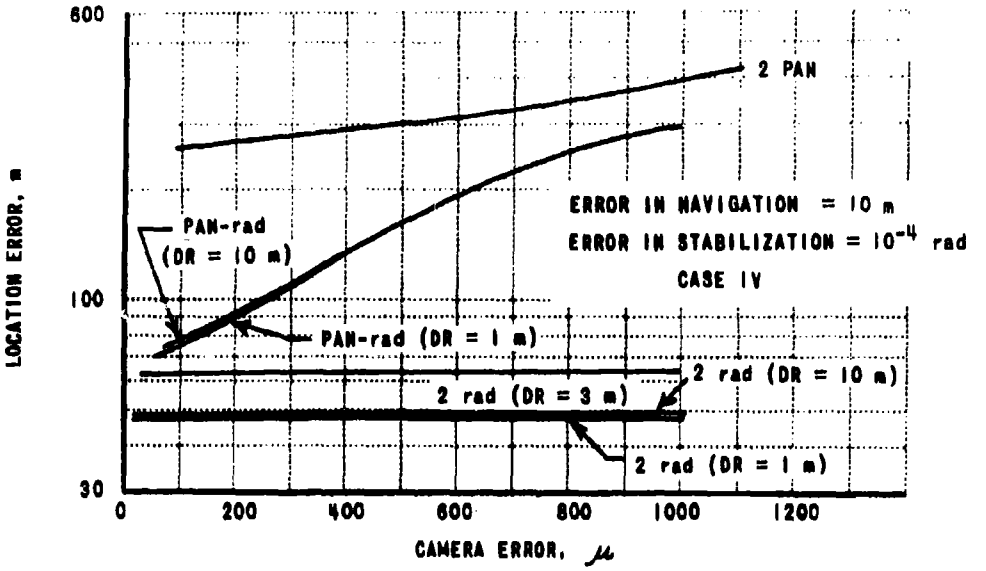

Figure 5.36 TARGET LOCATION ERROR

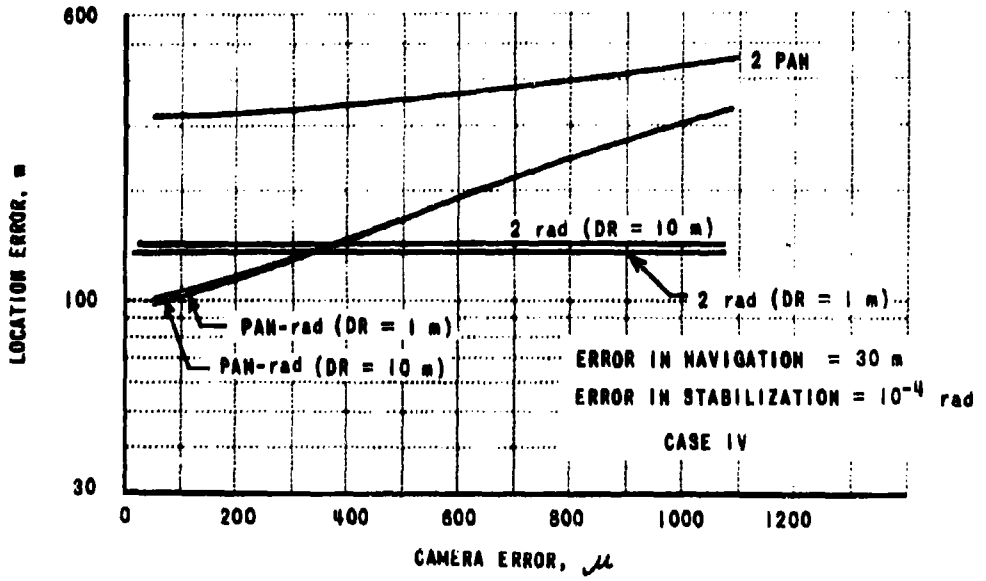

Figure 5.37 TARGET LOCATION ERROR

6. CONCLUSIONS

Although the study is primarily concerned with target location and charting, important conclusions about image registration must be included:

a) For the altitude range of boost-glide vehicles considered here, relief displacement errors in single images prevent registration of all except large targets. Even where stereo methods are used point location errors are still too large for images to be registered by only rectification* of the images. Improvement can be achieved only by identifying several points on each stereo model and forcing a local matching.

Conclusions concerning target location and charting:

b) Navigation errors in excess of about 30 meters cause all systems to be limited by that error. If inherent sensor capabilities are not to be overwhelmed by navigation errors, present systems require the aid of ground control data or control extension techniques.

c) As in the case for photographic systems, the best geometry for radar stereo** systems is that which causes the lines from the two sensors to the target to meet at right angles. For a camera-radar combination, the best geometry occurs with the two sensors carried in one vehicle. If both sensors are carried in one vehicle, such a combination can outperform other target location systems.

d) Stabilization errors do not appreciably affect low altitude systems, if present stabilization errors are assumed. At higher altitudes, stabilization errors can dominate in photographic systems.

---

* Rectification includes all corrections which can be made by calibration or calculation. For example, scale variation over the field, lens distortion and some static atmospheric effects are corrected during this process.

** Stereo is used in the broad sense defined at the start of Part I of this report.

e) When a large base line (separation of sensor stations) is available, as when separate flights or convergent photography is used, photographic stereo provides the most accurate target location.

f) Since radar is essentially independent of stabilization, and trilateration with radar stereo is only slightly dependent on relative positions of the two sensors, a trade-off point exists between radar and photographic stereo systems. The radar system outperforms the photographic system if navigation and stabilization errors are large.

7. RECOMMENDATIONS

The present study provides a comparison of the capabilities of sensor combinations for given values of error due to various sources. This study evaluates target location error in terms of basic target location equations.

Image registration by rectification* only has been shown to be impractical, even if stereo models are prepared first. Two other possibilities should be studied. First, the improvement possible by identifying points on each model and forcing these corresponding points to register should be investigated. Such local scale-changing might register the images quite well over the area surrounding the identifiable points. Secondly, other possible uses of less precise registration could be studied. For example, radar could be used for target detection, and a coarse image registration would allow a small area of a photograph to be isolated, with the target known to be within this area.

Research to improve navigation systems should be continued, since present navigation errors limit sensor capabilities.

Further study should be carried out to determine the precise reduction of target location error when redundant information is included as well as when control extension techniques are used. Such study could follow the outline of the least squares analysis presented in this report, but should include control extension.

* See first footnote, p. 51

PART II

8. ATMOSPHERIC EFFECTS

The probable contributions to target location errors due to atmospheric effects can be treated analytically and evaluated numerically if a few constants are obtained from experimental data. Steady refraction effects need not contribute to location errors, since they can be evaluated and taken into account in correcting photographic measurements for systematic errors (rectification). Fluctuations in atmospheric refraction, and random errors in evaluating steady effects are accounted for in the target location error analysis in Part I. In the following, all refraction effects are treated analytically, and numerical estimates are made on the basis of available data.

Refraction effects in airborne photographic systems result from the following density gradients in the earth's atmosphere and in the flow field associated with the airborne vehicle:

1. The hydrostatic density gradient in the ambient atmosphere due to the earth's gravitational field;
2. Heating effect gradients in the ambient atmosphere or in the flow field;
3. The density jump across the shock wave accompanying a supersonic aircraft;
4. The density gradient associated with the steady, continuous pressure distribution in the flow field related to the vehicle shape, attitude, and flight conditions;
5. Random density fluctuations associated with turbulence in the boundary layer or in the ambient atmosphere.

The resulting degradation of the photographic image can be described in terms of the following phenomena:

1. Displacement of the image by steady, uniform deflection of all the image forming rays;
2. Warping of the image by steady but non-uniform deflection of the image forming rays;

3. Shimmy or random motion of the image points by unsteady but uniform deflection of the rays;

4. Distention or image point spread by unsteady and non-uniform deflection of the rays;

5. Twinkling or brightness fluctuations due to random deflection at a considerable distance from the camera;

6. Dispersion or separation of colors, either steady or random, due to the spectral dependence of the specific refractivity.

The various refraction effects will be treated in the order listed, starting with the hydrostatic density gradient.

8.1 Hydrostatic Gradient

The relation between the variation of the index of refraction and the resulting deviation is given by the curvature equation, Reference 1,

$$t_{i,j}\, t^j = \frac{1}{n}\left(n_{,i} - n_{,j}\, t_i\, t^j\right) \qquad 8\text{-}1$$

where t^i is the direction vector tangent at any point to the image forming light ray passing through that point and $t_{i,j}\, t^j$ is the curvature of the ray. For most purposes the index of refraction n can be expressed in terms of a constant specific refractivity K, References 2, 3, 4, 5,

$$n = 1 + K\rho \qquad 8\text{-}2$$

where

$$K = .23 \text{ cm}^3/\text{gm} = .12 \text{ ft}^3/\text{slug}$$

For aerial photography of the ground from altitudes below 300,000 feet the direction of the vertical varies less than 10° along the ray from any visible point on the ground to the aircraft so that, for practical purposes, the earth can be treated as flat, the hydrostatic density gradient as unidirectional, and Snell's law can be used to describe the angular displacement ϵ at the airplane of the corresponding level displacement d along the ground by the

equation

$$\frac{\epsilon h}{\tan \alpha_c} = \frac{d \cos^2 \alpha_c}{\tan \alpha_c} = \rho_\alpha \sum_{i=1}^{m} A_i I_1^i - \sum_{i=1}^{m} A_i I_2^i \qquad 8\text{-}3$$

where ρ_α is the ambient density at the aircraft altitude, the summation is over the layers of constant lapse rate $L(h)$ from the ground to the aircraft, A_i are the coefficients

$$A_i = \frac{K T_i}{c_i \rho_i^{L_i/c_i}} \qquad 8\text{-}4$$

and I_1^i and I_2^i are the integrals

$$I_1^i = \int_{\rho_i}^{\rho_{i+1}} \rho^{\frac{L}{c}-1} d\rho = \log_e \frac{\rho_{i+1}}{\rho_i} \quad \text{if } L = 0$$

$$= \frac{c_i}{L}\left(\rho_{i+1}^{L/c} - \rho^{L/c}\right) \quad \text{if } L \neq 0 \qquad 8\text{-}5$$

and

$$I_2^i = \int_{\rho_i}^{\rho_{i+1}} \rho^{L/c} \, d\rho = \frac{c_i}{L_i + c_i}\left(\rho_{i+1}^{\frac{L}{c}+1} - \rho_i^{\frac{L}{c}+1}\right) \qquad 8\text{-}6$$

The reference values and coefficients for the ARDC Model Atmosphere, 1959 are given in Table 8.1 and the generalized displacement expressed in Equation 8-3 is plotted in Figure 8.1.

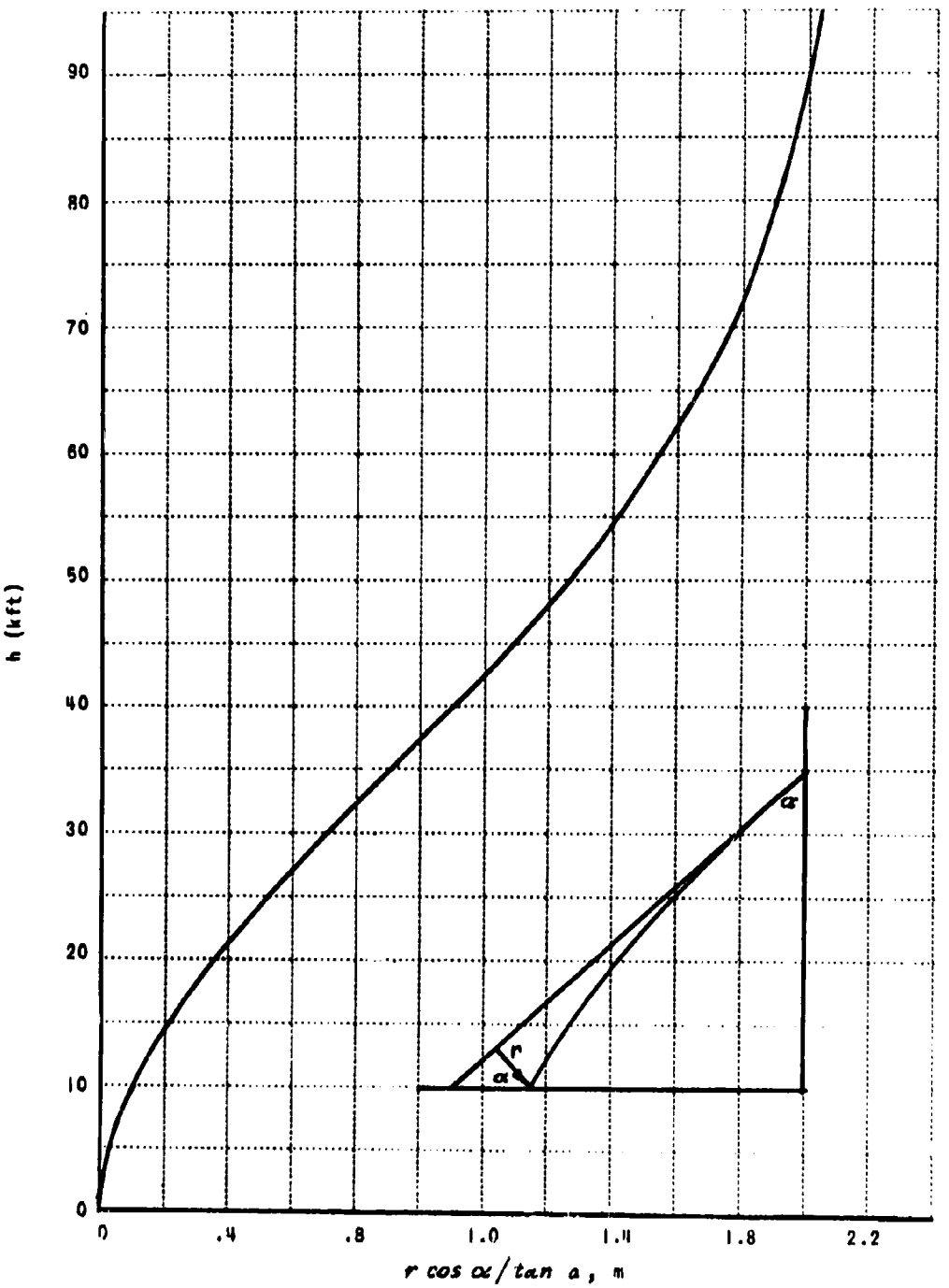

Figure 8.1 HYDROSTATIC DISPLACEMENT

TABLE 8.1

THE ARDC MODEL ATMOSPHERE, 1959

(Reference 6)

h_i (Kft)	$L \times 10^3$ (°R/Kft)	T_i (°R)	ρ_i (slug/ft^3)	g (lb/slug)	c_i (°R/Kft)	L_i/c_i	A_i
0	3.59	519	2.377×10^{-3}	32.17	15.13	.237	17350
36	0	390	7.055×10^{-4}	32.06	18.62	0	2520
82	-1.63	390	7.761×10^{-5}	31.92	20.16	-.081	1080
155	0	509	2.883×10^{-6}	31.70	18.43	0	3310
175	2.85	509	1.396×10^{-6}	31.64	15.52	.184	46700
249	0	298	8.131×10^{-8}	31.42	18.23	0	1960
300		298	4.256×10^{-9}	31.27			

Deflection of the light rays by the hydrostatic density gradient is steady and results in a radial warping about the nadir point. Since the displacement is positive, targets will be closer to the nadir point than indicated by the straight line tangent to the light ray at the camera or the image is expanded radially from the image of the nadir point.

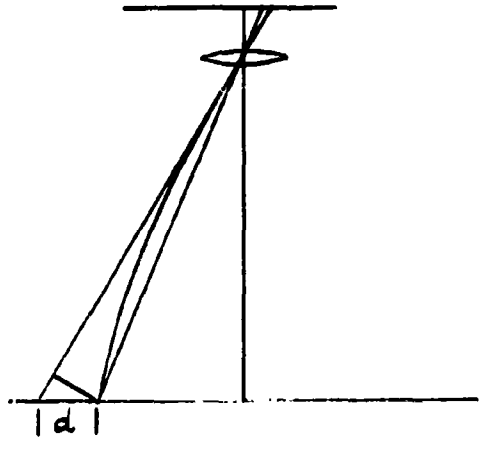

8.2 Temperature Effects

The boundary layer around an aircraft and thermal convection currents in the atmosphere are regions of nonuniform temperature but nearly uniform pressure where the density varies inversely with the temperature. The relatively steady temperature gradients in the atmosphere are small and have little effect on light rays while very high temperatures are reached at the skin of hypersonic vehicles and the resulting variation in refractivity may significantly deflect rays reaching the boundary layer with a high angle of incidence.

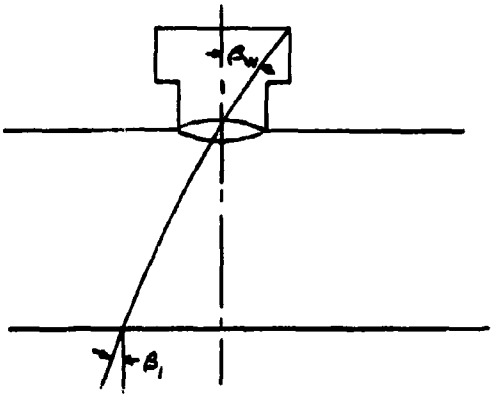

At the high supersonic velocities for which this deflection is most appreciable the temperatures at the wall becomes so high and the density so low that the refractivity $n-1$ at the wall vanishes and the variation of refractivity across the boundary layer is nearly to its value outside the boundary layer.

Then

$$\epsilon = \delta = K\rho_1 \tan\beta_1 \qquad 8\text{-}7$$

The effect of this deflection on the photographic image is a combination of displacement and warping depending on the range of the angle of incidence β_1 over the field of view. The deflection and displacement are positive indicating a stretching of the image. For turbulent boundary layers, the random effects of shimmy and distention can be treated as superimposed independent effects. These will be treated later.

8.3 Shock Wave

For the case of a shock wave the upstream and downstream angles of incidence, β_1 and β_2 respectively, are related by the expression

$$\frac{\sin\beta_2}{\sin\beta_1} = \frac{n_1}{n_2} \cong 1 - D \qquad 8\text{-}8$$

where the deflection modulus D is defined by the expression

$$D = K\rho_1 \left(\frac{\rho_2}{\rho_1} - 1\right) \qquad 8\text{-}9$$

and where second order terms in the refractivity are neglected.

But sin β_2 can be expressed as a function of β_1 and the deflection

$$\delta = \beta_2 - \beta_1$$

by the series expansion

$$\sin\beta_2 = \sin\beta_1 + \delta\cos\beta_1 - \delta^2\frac{\sin\beta_1}{2!} - \delta^3\frac{\cos\beta_1}{3!} + \cdots$$

Then, neglecting second and higher order terms in the small angle δ we have

$$\frac{\sin\beta_2}{\sin\beta_1} = 1 + \delta\cot\beta_1$$

from which

$$\delta = -D\tan\beta_1 \qquad 8\text{-}10$$

The angle of incidence β_1 depends on the viewing angle and the orientation of the shock wave. The normal to the shock and the upstream and downstream light rays are coplanar and it is in this plane that the angles of incidence and the deflection are measured. The shock wave angle, however, is measured in the plane of the normal to the shock and the aircraft velocity vector. In the simplest case, these two planes coincide and the angle of incidence β_1 is related to the shock wave angle θ_W with respect to the horizontal and the viewing angle α with respect to the vertical by the expression $\beta_1 = |\theta_W - \alpha|$ where the view angle α is positive for viewing forward, negative for rearward, while the angle of incidence and deflection modulus D are positive and, consequently, the angular deflection δ is always negative, i.e., the upstream angle of incidence is greater than the downstream and the image is compressed. The geometry for shock waves of general orientation is more involved but the calculations are straightforward and the details are omitted here.

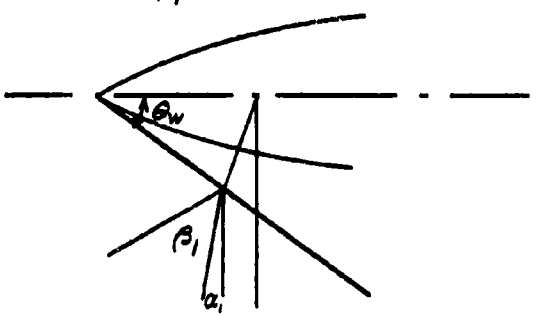

At low supersonic Mach numbers, the shock wave does not lie back along the body but is nearly perpendicular to the line of flight. In this case, some rays may cross the shock in the manner already described, some of the rays from the rear may reach the camera without crossing the shock, and some rays may be reflected to the camera from the downstream side of the shock. A further complication is the presence of the trailing shock wave caused by the convergence of the air behind the vehicle. Expressions are available, Reference 7, for finding the strength, shape, and distance between these shock waves but the results are mainly qualitative and more useful in determining the optimum camera placement and flight speed rather than in predicting the position and extent of the distortion bands on the photograph.

8.4 Flow Field

Between the body of a supersonic aircraft and its shock wave, there is a region in which the pressure, density, and fluid velocity vary smoothly and continuously. The distribution of these flow quantities throughout the field depends on the shape and velocity of the aircraft and on the ambient atmospheric conditions. A discussion of the techniques for calculating the density distribution in such a field is too involved to be included here except to mention, as an example, the method of characteristics. This method is one of the most accurate and useful approaches to finding the field quantities for supersonic, two-dimensional or axially symmetric flow and three-dimensional effects can be included as superimposed cross flow effects. The solution consists of two families of intersecting characteristic curves and the values of the flow quantities at the intersections. If these curves are plotted and the value of the density given at each intersection, curves of constant density can be faired across these curves and the density gradient estimated on the basis of the direction of and distance between these isochors. Then the deflection can be computed as the product of the specific refractivity K, the average perpendicular component of the density gradient, and the length of the path. Again, this deflection occurs so close to the camera that the angular displacement can be set equal to the angular deflection.

8.5 Random Fluctuations (Turbulence)

To treat random density fluctuations statistically, we will assume that turbulent regions in the atmosphere and the turbulent boundary layer around an aircraft are homogeneous and isotropic, i.e., that the statistical quantities are uniform throughout and independent of direction. These conditions, of course, are not realized since the size, strength, and orientation of the eddies depends partly on the flow velocity gradient which is certainly neither uniform nor isotropic, but, to a first approximation, the assumption is not too unreasonable.

A light ray in a region of turbulent density fluctuations can be pictured as a sinuous curve wriggling around in a very small turbular region which surrounds the mean path but which has no sharply defined boundary since the displacement of the ray from its mean position is described by a probability distribution. The instantaneous curvature relation can be expressed in the form

$$\delta_{i,j}\,\bar{t}^{j} = \eta_{,i} - \eta_{,j}\,\bar{t}_{i}\,\bar{t}^{j} \qquad 8\text{-}11$$

where the random curvature $\gamma_i = \delta_{i,j}\,\bar{t}^{j}$ as well as the deflection $\delta^{i} = t^{i} - \bar{t}^{i}$ and fluctuation $\eta = \frac{n-\bar{n}}{\bar{n}}$ are random quantities while the bars indicate statistical means.

The random distribution of density inhomogeneities is best discribed in terms of a correlation function

$$\psi(\xi) = \frac{\overline{\eta(x_1^{i})\,\eta(x_2^{i})}}{\overline{\eta^{2}}} \qquad 8\text{-}12$$

where ξ is the distance between the two points x_1^{i} and x_2^{i}. Without justification except that it has the value $\psi(0) = 1$ and slope $\psi'(0) = 0$ at $\xi = 0$, decreases monotonically to $\psi(\infty) = 0$, and seems intuitively to describe the expected distribution, we shall use the exponential function

$$\psi(\xi) = e^{-\xi^{2}/\xi_{0}^{2}} \qquad 8\text{-}13$$

where the reference value ξ_0 is $\sqrt{2}$ times the inflection valuc and is characteristic of the turbulent structure. With this correlation, the mean square

deflection of a ray passing through a homogeneous, isotropic turbulent layer of thickness s , turbulent scale ξ_0 , and mean square density fluctuation

$$\overline{\Delta^2\rho} = \overline{(\rho - \bar{\rho})^2} = \frac{\bar{n}}{K}\overline{\eta^2} \qquad 8\text{-}14$$

is given by the expression

$$\overline{\delta^2(s)} = 4K\,\overline{\Delta^2\rho}\left(\frac{s\sqrt{\pi}}{\xi_0} - 1\right) \qquad 8\text{-}15$$

The corresponding displacement η of an image point is

$$r_i = s_i\epsilon$$

where s_i is the image distance which, by the lens law, is related to the object distance s_0 and the focal length f by the equation

$$s_i = \frac{s_0 f}{s_0 - f}$$

and ϵ is the angular displacement at the camera,

$$\epsilon = \frac{(s_0 - s_t)\delta}{s_0}$$

where s_t is the distance from the camera to the turbulent layer. Then

$$\sqrt{\overline{r_i^2}} = \left(\frac{s_0 - s_t}{s_0 - f}\right) f\sqrt{\overline{\delta^2}}$$

For the turbulent boundary layer, the ratio in parentheses is very nearly unity and the angular displacement is equal to the deflection while, for a turbulent layer in the atmosphere, the quantity in parentheses is nearly equal to the ratio of the altitude of the turbulent layer h_t to the altitude of the camera h ,

$$\sqrt{\overline{r^2}} = f\sqrt{\overline{\delta^2}} \qquad \text{for a turbulent boundary layer} \qquad 8\text{-}16$$

$$= \frac{h_t}{h} f\sqrt{\overline{\delta^2}} \qquad \text{for an atmospheric boundary layer} \qquad 8\text{-}17$$

Because the structure of turbulence in the atmosphere is not homogeneous, it is necessary, at least for high altitude observation aircraft, to consider the atmosphere as consisting of several turbulent layers. The mean square angular displacement is then related to the mean square deflections by the equation

$$\overline{\epsilon^2}h^2 = \overline{\delta_1^2}h_1^2 + \overline{\delta_2^2}h_2^2 + \cdots$$

since the mean cross terms $2\,\overline{\delta_1 \cdot \delta_2}\, h_1 h_2$ vanish. Then the rms angular displacement is

$$\sqrt{\epsilon^2} = \frac{1}{h}\sqrt{\delta_1^2 h_1^2 + \delta_2^2 h_2^2 + \cdots}$$

and the rms image point displacement,

$$\sqrt{r^2} = \frac{f}{h}\sqrt{\sum_i (\delta^2 h^2)_i} \qquad 8\text{-}18$$

where $\sqrt{\delta_i^2}$ is the rms deflection due to layer i and h is the altitude of the midpoint of the layer.

These expressions describe the deflection and the displacement in the image plane of a single ray. But, unless the aperture of our camera lens is small compared to the characteristic size of the density inhomogeneities, we are concerned with refraction of a beam of essentially parallel rays rather than a single isolated ray. Although the random deflection of a single ray is the same whether there are other rays present or not, the instantaneous deflection of all the rays is partially correlated.

The correlation function $R\left(\frac{a}{\zeta_0}\right)$ describing the correlated deflection of rays passing through a circular aperture of radius a is given by the expression

$$R\left(\frac{a}{\zeta_0}\right) = \sum_{k=0}^{\infty} (-1)^k \frac{(2k+2)!\left(\frac{a}{\zeta_0}\right)^{2k}}{k!(k+1)!(k+2)!} \qquad 8\text{-}19$$

In the limit as the aperture radius approaches zero $R\left(\frac{a}{\zeta_0}\right)$ goes to unity and the instantaneous average deflection covariance is equal to the mean square deflection so that the image of a point source becomes, for an ideal system, a point moving over the circular region while for large apertures the deflections of widely spaced rays are uncorrelated and the image of a point tends to become a distended blur. The correlation function $R\left(\frac{a}{\zeta_0}\right)$ then expresses that part of the mean square deflection responsible for shimmy, i.e., motion of the image point, so that $R\left(\frac{a}{\zeta_0}\right)$ is called the shimmy factor and plotted in Figure 8.2.

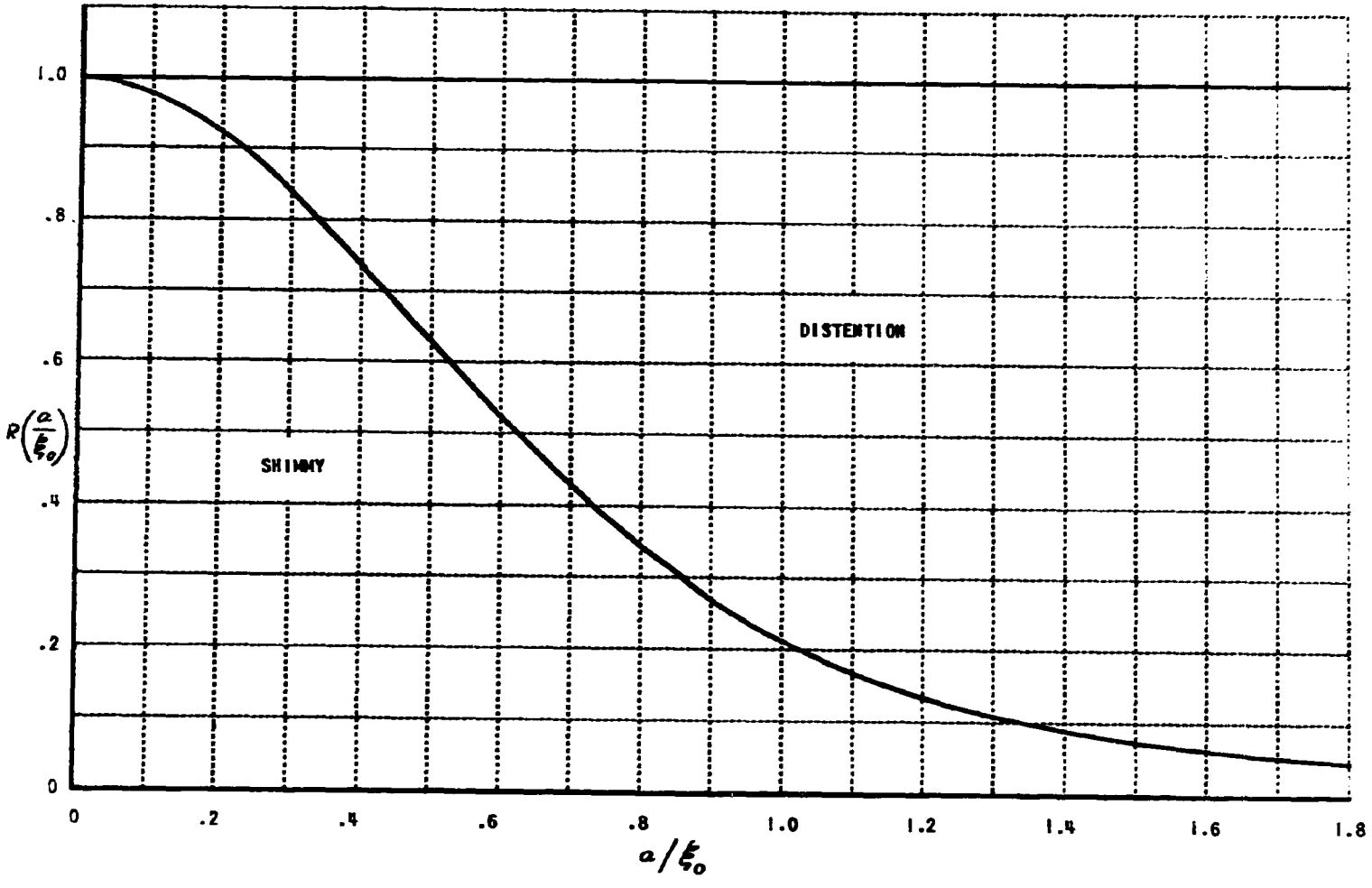

FIGURE 8.2 SHIMMY FACTOR $R\left(\frac{a}{\xi_0}\right)$

Besides shimmy and distention, there is the effect of twinkle due to refraction by density inhomogeneities so far from the camera that the linear displacement of the rays at the camera is more significant than the deflection. The relative magnitudes of these effects depend on the aperture as well as the relative distances from the camera to the turbulence and the object photographed and can be described in terms of the quantity,

$$\frac{\sqrt{\overline{r^2}}/f}{\sqrt{\overline{d^2}}/ah} = \frac{a \cdot h_t}{h - h_t} \qquad 8\text{-}20$$

where d is the linear displacement of the ray at the camera.

Considerable twinkle is indicated when $\sqrt{\overline{d^2}}$ is of the same order of magnitude or greater than the radius a. As an example, consider an rms deflection of .02 milliradian due to turbulence at 20,000 feet, a focal length of 1 foot, and an aircraft altitude of 40,000 feet. Then the resulting rms image displacement is

$$\sqrt{\overline{r^2}} = \sqrt{\overline{\delta^2}}\,\frac{h_t}{h} = 10^{-5}\ \text{ft.}$$

which is generally negligible while the displacement of the ray at the objective lens is

$$\sqrt{\overline{d^2}} = \delta(h - h_t) = 0.4\ \text{ft.}$$

which, for most camera apertures, indicates considerable twinkle.

8.6 Conclusions

The relative importance of the various factors contributing to the degradation of photographic images due to refraction effects in the atmosphere and flow field is indicated by Figure 8.3.

In these curves, the most questionable data concerns the structure and location of turbulence in the atmosphere and the eddy strengths and distribution in turbulent boundary layer. The values indicated, i.e., $\sqrt{\Delta^2 T_{atm}} = 1^\circ R$, $\xi_{o_{atm}} = 1\ ft$, $\sqrt{\Delta^2 \rho_{b.l.}} = \frac{1}{8}\rho_1$, and $(s/\xi_o)_{b.l.} = 10$, were chosen because they are representative and are easily extrapolated to suit other conditions. Since deflection by the shock wave is proportional to $(\rho_2/\rho_1) - 1$ and $\tan\beta^*$, values were chosen for ρ_2/ρ_1 and β so that these values can be conveniently extrapolated. While these values are representative they cannot be associated with a particular velocity, body shape, or vehicle attitude because

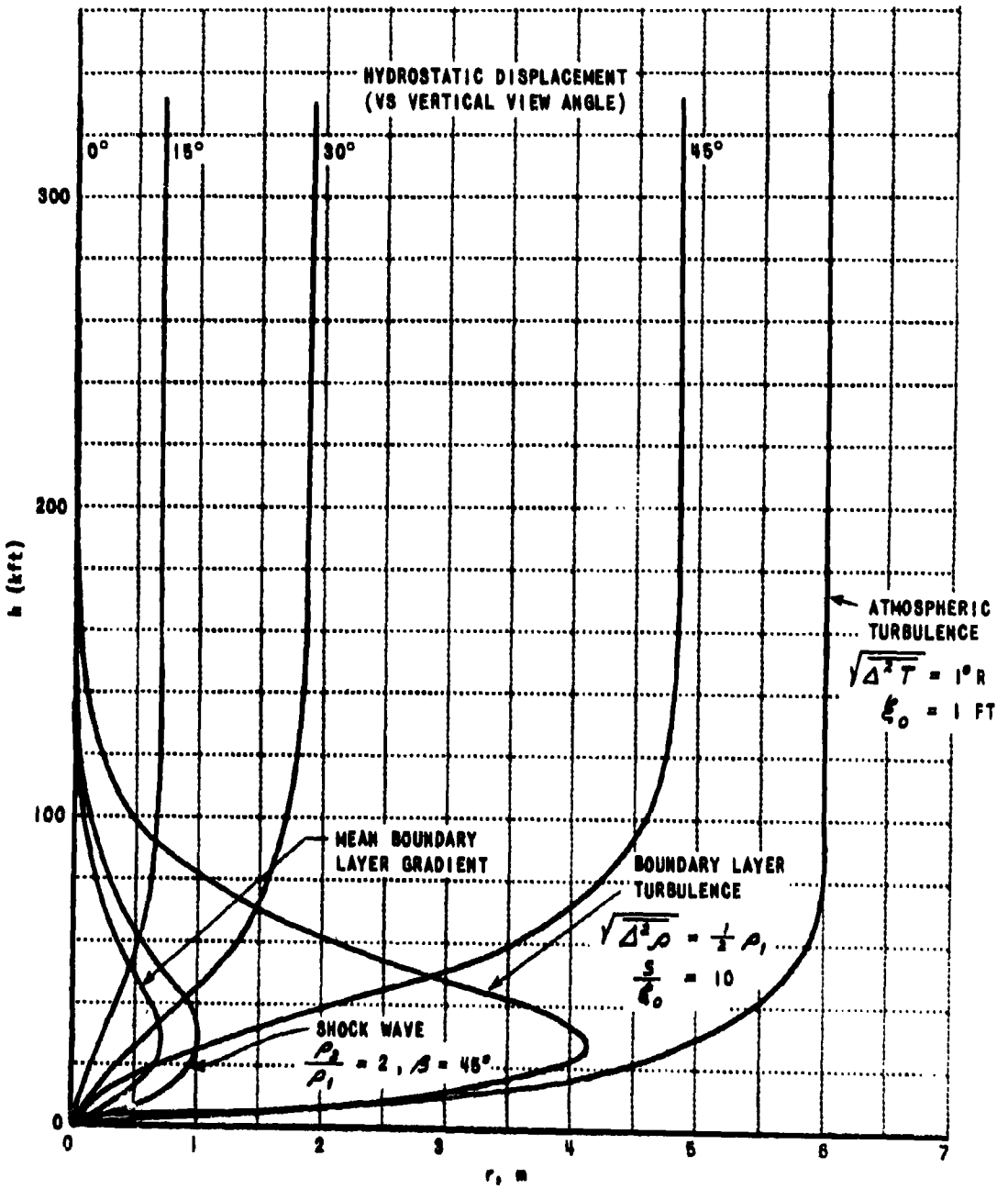

Figure 8.3 REFRACTION EFFECTS OF FLOW FIELD AND ATMOSPHERE
LINEAR DISPLACEMENT VS ALTITUDE

of the involved interdependence between these quantities. The deflection by the mean boundary layer gradient is represented by a curve based on hypersonic velocities. However the variation with velocity is not linear so that this curve is representative of most practical vehicles.

REFERENCES

1. Advanced Target Location System, Final Report Cornell Aeronautical Laboratory, Inc. 15 July 1960 Section 4, Appendices 4A and 4B SECRET

2. Barrell, H., and Sears, J.E. Phil. Trans. Roy. Soc. London, A-238 (1940) 1-64, The Refraction and Dispersion of Air for the Visible Spectrum

3. Edlen, B. Jour. Opt. Soc. Am. 43/5 (May 1953) 339-344, The Dispersion of Standard Air

4. Rank, D.H., and Shearer, J.N. Jour. Opt. Soc. Am. 44/7 July 1954 575 (L), Index of Refraction of Air in the Infrared

5. Essen, L., and Froome, K.D. Proc. Phys. Soc. B-64 (1951) 862-875 The Refractive Indices and Dielectric Constants of Air and its Principal Constituents at 24000 Mc/s

6. Minsner, R.A., Champion, K.S.W., and Pond, H.L. Geophysics Research Directorate Air Force Cambridge Research Center, Air Force Surveys in Geophysics No. 115, August 1959 The ARDC Model Atmosphere, 1959

7. Nielsen, J.N., et al, Vidya, Inc. Report No. 12 August 1959 The Effects of Supersonic and Hypersonic Aircraft Speed upon Aerial Photography

8. Brown, D.C. RCA Data Reduction Tech Rep # 39 20 August 1957 AFMTC-TR-57-22 Astia Document # 124144

GLOSSARY OF SYMBOLS

Non-Stereo Systems

NP = target offset measured along spherical earth

NP' = target offset measured along flat datum (for camera)

NP'' = target offset measured along flat datum (for radar)

E_c = target offset error for camera

E_R = target offset error for radar

R_E = earth radius

H = altitude of sensor above earth datum

θ = angular offset of target

h = target altitude above earth reference datum

Y = target offset along earth reference datum

Stereo Systems

$\vec{P}$ = vector from base to target

$\vec{S}_{(n)}$ = vector from base to sensor (n)

$\vec{R}_{(n)}$ = vector from sensor (n) to target

$\vec{S}$ (no subscript) = vector from sensor 1 to sensor 2

m_j = the j th measured variable in a list of measured quantities

$d(*)$ = the error in the quantity called *

dX = combined film measurement errors (microns)

dF = focal length measurement error (microns)

dN = combined navigation errors (all components of error vectors)

$dSTAB$ = combined angular errors in all orientation measurement (stabilization)

dR = radar range measurement error

$C_{(i)}$ = error contribution due to ith error source

$H_{(n)}$ = altitude of sensor (n) above reference coordinate origin

A = angular offset of target from sensor 1

$F_{(n)}$ = focal length of camera (n)

$a_{(*)}$ = partial derivation of target position vector with respect to variable (*).

$C.E.$	=	camera error
l, s	=	film coordinates
T_{ij}	=	transformation from system j to system i
ψ, θ, ρ	=	yaw, pitch and roll angles
$(\hat{w})$	=	unit vector
LO	=	change in longitude from sensor 1 to sensor 2
LA	=	change in latitude from sensor 1 to sensor 2
AZ	=	change in flight heading from sensor 1 to sensor 2
U	=	$R_1 - (\hat{R}_1 \cdot \vec{S})$
A, B, C, D, E, M	=	intermediate quantities defined in Appendix C for convenience during radar analysis
x_p, y_p, f	=	film coordinates and focal length in frame camera
α	=	parameter for length of camera to target vector
r, σ, E	=	spherical coordinates of target with respect to radar sensor
$\vec{v}$	=	residuals of least squares adjusted measurements
$\vec{T}$	=	vector of parameters for least squares adjustment
$\vec{\delta}$	=	vector of parameter residuals after adjustment
σ^2	=	variance matrix
ω_i	=	weight of the ith measurement
$\vec{F}$	=	condition equation vector of measured values
a_{ij}, b_{ik}	=	matrices of derivatives of $\vec{F}$
$\vec{\lambda}$	=	vector of Lagrange multipliers
S	=	weighted sum of squares of residuals

Atmospheric Effects

t_i	=	tangent vector to light ray
n	=	index of refraction
K	=	specific refractivity
ρ	=	density of atmosphere

GLOSSARY OF SYMBOLS (Contd.)

ϵ	=	angular displacement of ray
d	=	ground displacement of ray
α_c	=	angle away from vertical
T	=	temperature
L	=	lapse rate (dT/dh)
β	=	angle of incidence to boundary layer
δ	=	deflection of ray vector
D	=	deflection modulus
ξ	=	argument of correlation function
ψ	=	correlation function
ξ_o	=	turbulence scale
S	=	thickness of turbulent layer
r	=	image displacement
f	=	focal length of camera
$S_{(\cdot)}$	=	distance (subscript i for image, o for object)
a	=	aperture radius of lens
R	=	shimmy factor
h	=	altitude

APPENDIX A

STEREO PANORAMIC CAMERA ERROR ANALYSIS

The triangulation equations for basic target location will be derived in this appendix for location by two panoramic cameras. Two frame cameras can be handled by an almost identical analysis. The errors in the target position vector will be evaluated as functions of the measurement errors by differentiation of the target location equations.

A. 1 Derivation of Target Location Equations

Each camera station from which a photograph is taken provides measurements of two film coordinates and a focal length, which combine to determine a direction in space from the camera to the target. Effectively, this fixes azimuth and zenith angles but without range information. With two photographs, from different stations, the target location is over-determined, since four quantities are known where three are needed. The solution given here for the basic target location is derived using equation 4-2 of Section 4 (repeated below) as a starting point. The overdetermination is eliminated mathematically by using only the minimum number of equations sufficient to determine the target location. Physically, the solution of these equations is the distance from one camera to the point of closest approach of the target position vectors from the two cameras. This point of closest approach is, of course, the intersection of the lines, if they meet. Repeating equation 4-2:

$$\vec{R}_1 = \vec{R}_2 + \vec{S} \tag{4-2}$$

The vector equation, 4-2, implies three scalar equations. Rather than using the Cartesian components, a better solution can be obtained by taking scalar products with the unit vectors determined by the cameras. Thus, if $\hat{R}_1$ is a unit vector whose direction is fixed by camera number 1, and $\hat{R}_2$ is the same for camera 2, scalar products yield:

$$\vec{R}_1 \cdot \vec{R}_1 = R_1 = (\hat{R}_1 \cdot \hat{R}_2) R_2 + \vec{S} \cdot \hat{R}_1 \tag{A-1}$$

$$\vec{R}_2 \cdot \vec{R}_1 = R_1 (\hat{R}_1 \cdot \hat{R}_2) = R_2 + \vec{S} \cdot \hat{R}_2$$

Since only two of the three possible equations are used, the overdetermination is eliminated. The magnitude of R may be solved from equation A-1, as:

$$R_1 = \frac{\vec{S} \cdot \hat{R}_1 - (\vec{S} \cdot \hat{R}_2)(\hat{R}_1 \cdot \hat{R}_2)}{1 - (\hat{R}_1 \cdot \hat{R}_2)^2} \qquad \text{A-2}$$

The target location, $(\vec{R}_1)$, is specified by the magnitude, R_1, and the direction $\hat{R}_1$ with respect to camera station 1, as:

$$\vec{R}_1 = R_1 \hat{R}_1 \qquad \text{A-3}$$

A. 2 Evaluation of Position Vector Errors

The error in $\vec{R}_1$ due to an error in variable w_j is found by differentiating. The result is:

$$\frac{\partial \vec{R}_1}{\partial w_j} = \left(\frac{\partial R_1}{\partial w_j}\right) \hat{R}_1 + R_1 \left(\frac{\partial \hat{R}_1}{\partial w_j}\right) \qquad \text{A-4}$$

The errors in the target position vector can therefore be found if the errors in the unit vector and the errors in the vector magnitude are evaluated.

A. 3 Errors in the Unit Vector

The unit vector $\hat{R}_1$ can be written in terms of measured values of film coordinates (l, s) and focal length (f) for the panoramic camera by simply examining the geometry of the system, as shown in figure A-1. Then, in terms of sensor 1 coordinates:

$$\hat{R}_1 = -\frac{1}{(l^2 + F^2)^{1/2}} \begin{bmatrix} l \\ F \sin(s/F) \\ F \cos(s/F) \end{bmatrix} \qquad \text{A-5}$$

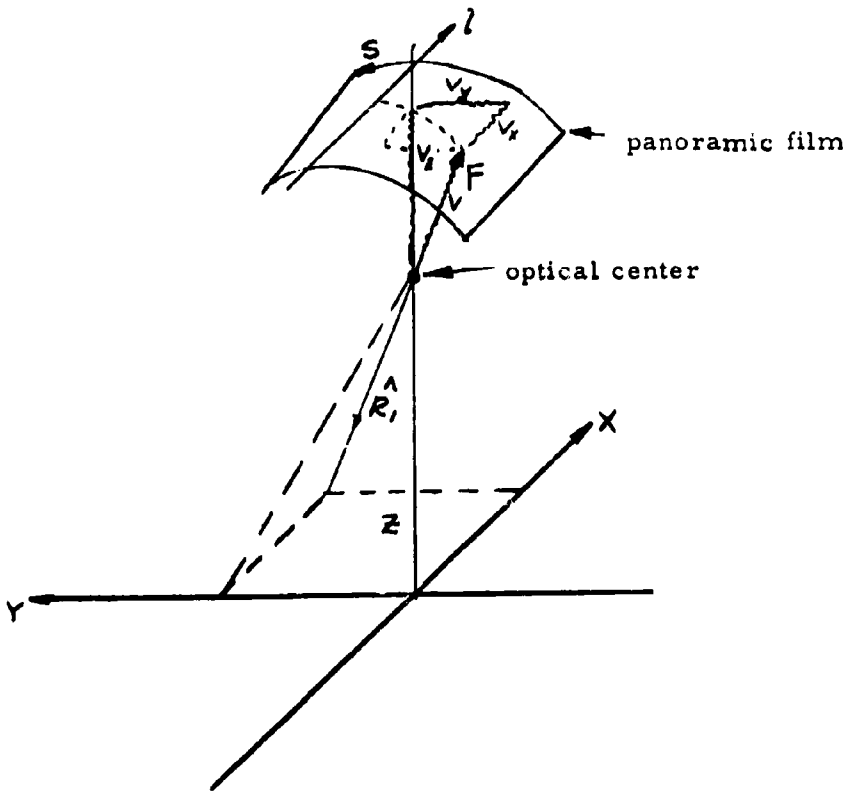

$$\hat{R}_1 = -\frac{\vec{V}}{|V|} \quad , \qquad |V| = (l^2 + F^2)^{1/2}$$

$$V = \begin{bmatrix} l \\ F \sin(s/F) \\ F \cos(s/F) \end{bmatrix}$$

Figure A. 1 PANORAMIC CAMERA GEOMETRY

But $\hat{R}_1$ must be known in earth fixed (base) coordinates. While the base coordinates can be chosen so that the mean value of roll, pitch and yaw angles is zero, there is error possible in these angles. The transformation matrix must be written out and differentiated. Writing roll, pitch and yaw as ρ, ϕ and ψ the matrix is:

$$T_{01} = \begin{bmatrix} \cos\psi & -\sin\psi & 0 \\ \sin\psi & \cos\psi & 0 \\ 0 & 0 & 1 \end{bmatrix} \begin{bmatrix} \cos\phi & 0 & \sin\phi \\ 0 & 1 & 0 \\ -\sin\phi & 0 & \cos\phi \end{bmatrix} \begin{bmatrix} 1 & 0 & 0 \\ 0 & \cos\rho & -\sin\rho \\ 0 & \sin\rho & \cos\rho \end{bmatrix} \qquad \text{A-6}$$

When only the measured value is needed, it can be taken as:

$$T_{01} = \begin{bmatrix} 1 & 0 & 0 \\ 0 & 1 & 0 \\ 0 & 0 & 1 \end{bmatrix} \qquad \text{A-7}$$

The error in $\hat{R}_1$ in base coordinates is then the error in $(T_{01}\hat{R}_1)$ where $\hat{R}_1$ is measured in sensor 1 coordinates. The error in $\hat{R}_1$ is therefore given by:

$$\left(\frac{\partial \hat{R}_1}{\partial \nu_j}\right)_{\substack{\text{base} \\ \text{coord.}}} = T_{01}\left(\frac{\partial \hat{R}_1}{\partial \nu_j}\right)_{\substack{\text{sensor 1} \\ \text{coord.}}} + \left(\frac{\partial T_{01}}{\partial \nu_j}\right)\hat{R}_1 \qquad \text{A-8}$$

where the products are matrix products.

For the error analysis, the measured variables for the system must be listed:

$\nu_1 = l_1$		$\nu_{10} = \rho_1$	sensor 1 orientation
$\nu_2 = S_1$		$\nu_{11} = \phi_1$	
$\nu_3 = F_1$		$\nu_{12} = \psi_1$	
$\nu_4 = S_x$	S_{2x}	$\nu_{13} = \rho_2$	sensor 2 orientation
$\nu_5 = S_y$	S_{2y}	$\nu_{14} = \phi_2$	
$\nu_6 = S_z$	S_{2z}	$\nu_{15} = \psi_2$	
$\nu_7 = S_{1x}$		$\nu_{16} = l_2$	sensor 2
$\nu_8 = S_{1y}$		$\nu_{17} = S_2$	
$\nu_9 = S_{1z}$		$\nu_{18} = F_2$	

The variables $\nu_{4,5,6}$ are dependent on how the navigation vector is measured. If both sensors are mounted on the same aerial platform, and the two sensor records are made during the same flight, then the navigation vector, $\vec{S}$ involves errors due only to the change of position during the interval between records. In that case, $\nu_{4,5,6}$ are the components of $\vec{S}$. If the sensor records are made from different platforms and therefore different flights, the vector $\vec{S}$ involves errors from the two navigation vectors $\vec{S}_2$ and $\vec{S}_1$ In that case $\nu_{4,5,6}$ are the components of $\vec{S}_2$. For one flight $\vec{S}$ is independent of errors in S_1 , while for two flights, $\vec{S}$ is given by:

$$\vec{S} = \vec{S}_2 - \vec{S}_1 \tag{4-3}$$

It is convenient to differentiate always with respect to components of $\vec{S}$, and take the change of dependent variables into account separately as:

$$\frac{\partial\ (\text{function})}{\partial\ S_i} = \frac{\partial\ (\text{function})}{\partial S_i} \tag{A-9}$$

$$\left.\begin{aligned} \frac{\partial\ (\text{function})}{\partial (S_2)_i} &= \frac{\partial\ (\text{function})}{\partial S_i}\left[\frac{\partial S_i}{\partial (S_2)_i}\right] \\ \frac{\partial\ (\text{function})}{\partial (S_1)_i} &= \frac{\partial\ (\text{function})}{\partial S_i}\left[\frac{\partial S_i}{\partial (S_1)_i}\right] \end{aligned}\right\} \text{ for 2 flights} \tag{A-10}$$

where $\frac{\partial S_i}{\partial (S_2)_i} = 1$, and $\frac{\partial S_i}{\partial (S_1)_i} = -1$ as follows, since $\vec{S} = \vec{S}_2 - \vec{S}_1$.

Therefore, derivatives with respect to S_i will be written as if $\nu_{4,5,6}$ were the components S_i and derivatives with respect to $\nu_{7,8,9}$ will be omitted from the list. The values of unit vector error may be computed in base coordinates by differentiating equations A-5 and A-6 and combining according to equation A-8. Omitting zero values, these are (l, s, and F refer to sensor 1):

$$\frac{\partial (\hat{R}_1)_z}{\partial \nu_i} = \left\{-1 + \frac{l^2}{(l^2 + F^2)}\right\} \frac{1}{(l^2 + F^2)^{1/2}} \tag{A-11}$$

$$\frac{\partial(\hat{R}_1)_x}{\partial \nu_3} = \frac{Fl}{(l^2+F^2)^{1/2}}$$

$$\frac{\partial(\hat{R}_1)_z}{\partial \nu_{11}} = \frac{-F\cos(s/F)}{(l^2+F^2)^{1/2}}$$

$$\frac{\partial(\hat{R}_1)_x}{\partial \nu_{12}} = \frac{+F\sin(s/F)}{(l^2+F^2)^{1/2}}$$

$$\frac{\partial(\hat{R}_1)_y}{\partial \nu_1} = \frac{lF\sin(s/F)}{(l^2+F^2)^{3/2}}, \qquad \frac{\partial(\hat{R}_1)_y}{\partial \nu_2} = \frac{-\cos(s/F)}{(l^2+F^2)^{1/2}}$$

$$\frac{\partial(\hat{R}_1)_y}{\partial \nu_3} = \left\{(s/F)\cos(s/F) - \sin(s/F) + \frac{F^2\sin(s/F)}{(l^2+F^2)}\right\}\frac{l}{(l^2+F^2)^{1/2}}$$

$$\frac{\partial(\hat{R}_1)_y}{\partial \nu_{10}} = \frac{F\cos(s/F)}{(l^2+F^2)^{1/2}}, \qquad \frac{\partial(\hat{R}_1)_y}{\partial \nu_{12}} = \frac{-l}{(l^2+F^2)^{1/2}}$$

$$\frac{\partial(\hat{R}_1)_z}{\partial \nu_1} = \frac{lF\cos(s/F)}{(l^2+F^2)^{3/2}}, \qquad \frac{\partial(\hat{R}_1)_z}{\partial \nu_2} = \frac{\sin(s/F)}{(l^2+F^2)^{1/2}}$$

$$\frac{\partial(\hat{R}_1)_z}{\partial \nu_3} = \left\{-[\cos(s/F) + (s/F)\sin(s/F)] + \frac{F^2\cos(s/F)}{(l^2+F^2)}\right\}\frac{l}{(l^2+F^2)^{1/2}}$$

$$\frac{\partial(\hat{R}_1)_z}{\partial \nu_{10}} = \frac{-F\sin(s/F)}{(l^2+F^2)^{1/2}}, \qquad \frac{\partial(\hat{R}_1)_z}{\partial \nu_{11}} = \frac{l}{(l^2+F^2)^{1/2}}$$

A.4 Errors in Position Vector Magnitude

The values of $[\ \partial R_1 / \partial \nu_j\ ]$ are derived by differentiating the equation for R_1 (A-2) with respect to each ν_j. Equation A-2 is rewritten with quantities grouped for convenience:

$$R_1 = \frac{A - BE}{1 - E^2} \qquad \text{A-12}$$

where:

$$A = \vec{S} \cdot \hat{R}_1$$

$$B = \vec{S} \cdot \hat{R}_2$$

$$E = \hat{R}_1 \cdot \hat{R}_2$$

Then, the derivatives of R_1 are:

$$\frac{\partial R_1}{\partial \nu_j} = \frac{1}{1 - E^2}\left\{\frac{\partial A}{\partial \nu_j} - E\,\frac{\partial B}{\partial \nu_j} + (2CE - B)\,\frac{\partial E}{\partial \nu_j}\right\} \qquad \text{A-13}$$

Where,

$$\frac{\partial A}{\partial \nu_j} = \vec{S} \cdot \frac{\partial \hat{R}_1}{\partial \nu_j} + \frac{\partial \vec{S}}{\partial \nu_j} \cdot \hat{R}_1 \qquad \text{A-14}$$

$$\frac{\partial B}{\partial \nu_j} = \vec{S} \cdot \frac{\partial \hat{R}_2}{\partial \nu_j} + \frac{\partial \vec{S}}{\partial \nu_j} \cdot \hat{R}_2 \qquad \text{A-15}$$

$$\frac{\partial E}{\partial \nu_j} = \hat{R}_1 \cdot \frac{\partial \hat{R}_2}{\partial \nu_j} + \frac{\partial \hat{R}_1}{\partial \nu_j} \cdot \hat{R}_2 \qquad \text{A-16}$$

With the above grouping, A, B, and E and their derivatives are scalars. However, the individual terms in the last three equations contain scalar products of vectors. Therefore, all of these vectors must be transformed to the same coordinate system. The logical system to choose is an earth fixed system. Since the target is being located by evaluating $\vec{R}_1$, the earth fixed system is chosen at sensor 1. These coordinates are the translated base coordinates already implicitly used in section 4, as well as for the computation of $[\ \partial \hat{R}_1 / \partial \nu_j\ ]$. Thus, $\hat{R}_1$ has been transformed

to this coordinate system, and $\vec{S}$ is measured in this system (any earth fixed system would do). Only $\hat{R}_2$ must be transformed. This transformation is done in two steps:

1. Transform from sensor 2 coordinates to earth fixed coordinates at sensor 2. This transformation is exactly to form of that used for R^2, and the values of $[\partial \hat{R}_1 / \partial \omega_j]$ can be used for $(\partial \hat{R}_2 / \partial \omega_j)$ if all reference to sensor 1 is replaced by sensor 2. Therefore, l, s and f are used from sensor 2, and ω_j ($j = 1$ to 3, 10 to 12) are replaced by ($j = 16$ to 18, 13 to 15)

2. Transform from earth fixed coordinates at sensor 2 to earth fixed coordinates at sensor 1. (The errors involved are due to navigation.)

The second transformation matrix depends on the relative orientation of the earth fixed systems at sensor 1 and sensor 2. The different orientation is due to the possibility of different flight directions, and to the change of direction of vertical across the surface of the earth. If the X direction at sensor 1 is called north, then a latitude and longitude can be connected to the components of the navigation vector using the usual definitions. The change in flight direction will be measured as an azimuth angle. These angles are:

$$\text{longitude} = LO = S_Y / R_E$$
$$\text{latitude} = LA = S_X / R_E \qquad \text{A-17}$$

azimuth = AZ = flight direction of sensor 2 with respect to 1, where R_E is the radius of the earth. Using (C) to mean (cos) and (S) to mean (sin), the transformation matrix is:

$$T_{02} = \begin{bmatrix} (CAZ)(CLA) & (SAZ)(CLA) & (SLA) \\ -(SAZ)(CLO)+(CAZ)(SLA)(SLO) & (CAZ)(CLO)+(SAZ)(SLA)(SLO) & -(CLA)(SLO) \\ -(SAZ)(SLO)-(CAZ)(SLA)(CLO) & (CAZ)(SLO)-(SAZ)(SLA)(CLO) & (CLA)(CLO) \end{bmatrix} \qquad \text{A-18}$$

Since error in flight direction has been taken into account in the first transformation, the value of $A\hat{Z}$ is known in this transformation, without error. The error in $\hat{R}_2$ is found in translated base coordinates as:

$$\left(\frac{\partial \hat{R}_2}{\partial \nu_j}\right)_0 = T_{02}\left(\frac{\partial \hat{R}_2}{\partial \nu_j}\right)_2 + \left(\frac{\partial T_{02}}{\partial \nu_j}\right)(\hat{R}_2)_2 \qquad \text{A-19}$$

The terms in this equation have been computed, except for $(\partial T_{02}/\partial \nu_j)$. The terms can be found:

T_{02} in equation A-18

$[\partial \hat{R}_2 / \partial \nu_j]_2$ use equation A-11, changing $\hat{R}_1$ to $\hat{R}_2$, and changing $j = 1, 2, 3$ to $j = 16, 17, 18$
$j = 10, 11, 12$ to $j = 13, 14, 15$

$[\hat{R}_2]_2$ use equation A-5, changing $\hat{R}_1$ to $\hat{R}_2$; l, s, f to l_2, s_2, f_2

The term $[\partial T_{02}/\partial \nu_j]$ contains errors due only to S_x and S_y (variables ν_4 and ν_5). These are (using the same notation as equation A-18):

$$\frac{\partial T_{02}}{\partial \nu_4} = \begin{bmatrix} -(CA\hat{Z})(SLA) & -(SA\hat{Z})(SLA) & (CLA) \\ (CA\hat{Z})(CLA)(SLO) & (SA\hat{Z})(CLA)(SLO) & (SLA)(SLO) \\ -(CA\hat{Z})(CLA)(CLO) & -(SA\hat{Z})(CLA)(CLO) & -(SLA)(CLO) \end{bmatrix} \qquad \text{A-20}$$

$$\frac{\partial T_{02}}{\partial \nu_5} = \begin{bmatrix} 0 & 0 & 0 \\ -(SA\hat{Z})(SLO) - (CA\hat{Z})(SLA)(CLO) & (CA\hat{Z})(SLO) - (SA\hat{Z})(SLA)(CLO) & (CLA)(CLO) \\ (SA\hat{Z})(CLO) - (CA\hat{Z})(SLA)(SLO) & -(CA\hat{Z})(CLO) - (SA\hat{Z})(SLA)(CLO) & (CLA)(SLO) \end{bmatrix} \qquad \text{A-21}$$

Because of the matrix multiplications for coordinate transformation, the equations would be overly lengthy if expressions for $[\partial R_1 / \partial \nu_j]$ were written out explicitly. In practice, when these values are computed, they are evaluated step by step, using the expressions already given. Equation A-19, with the above expressions, provides a value of $[\partial \hat{R}_2 / \partial \nu_j]$ and $\hat{R}_2$.

$[\ \partial \hat{R}_1 / \partial \nu_j\ ]$ and $\hat{R}_1$ are found from Equations A-11 and A-5. $[\ \partial R_1 / \partial \nu_j\ ]$ can be evaluated using Equations A-13 to A-16, plus:

$$\vec{S} = [S_x, S_y, S_z] \qquad \text{A-22}$$

and (omitting zero values):

$$\frac{\partial \vec{S}}{\partial \nu_4} = [1, 0, 0] \ , \ \frac{\partial \vec{S}}{\partial \nu_5} = [0, 1, 0]$$

$$\frac{\partial \vec{S}}{\partial \nu_6} = [0, 0, 1] \qquad \text{A-23}$$

A.5 Results

The values of $[\ \partial R_1 / \partial \nu_j\ ]$, $\hat{R}_1$, R_1, and $[\ \partial \hat{R}_1 / \partial \nu_j\ ]$ have been derived for photographic stereo in this appendix. These terms are used to provide the required list of values of $[\ \partial \vec{R}_1 / \partial \nu_j\ ]$ for Section 4.

APPENDIX B

PANORAMIC CAMERA WITH RADAR, ERROR ANALYSIS

In this appendix, the target location equations are derived for a panoramic camera combined with a side-looking radar. The values of $[\partial(\vec{R}_1) / \partial r_j]$ are derived by differentiation of the location equations.

B.1 Derivation of the Location Equations

The target is located by a combination of directional information provided by the camera, and range information provided by the radar. Since the two sensors are not necessarily at the same point, the solution is not the trivial, separated form given by that special case. Since azimuth information provided by radar is relatively low precision, only the range measurement is used in the basic location analysis. The solution therefore takes the form of finding the intersections of a sphere and a line, the sphere being the surface of constant range from the radar and the line being the direction fixed by the camera. Equation 4-2 of Section 4 is the basis for the derivation of the location equations. Repeating Equation 4-2:

$$\vec{R}_1 = \vec{S} + \vec{R}_2 \qquad (4\text{-}2)$$

The direction of $\vec{R}_1$ is known from camera measurements as given in Appendix A. Repeating the value of this unit vector ($\hat{R}_1$) for panoramic camera:

$$\hat{R}_1 = -(l^2 + F^2)^{-1/2} \begin{bmatrix} l \\ F \sin s/F \\ F \sin s/F \end{bmatrix} \qquad (A\text{-}5)$$

where: s, l are film coordinates

F = focal length

In Equation 4-2, repeated above, the direction of $\vec{R}_1$ is known ($\hat{R}_1$); $\vec{S}_1$, the navigation vector, is known; the magnitude of $\vec{R}_2$, (R_2), is measured by radar; and the magnitude of $\vec{R}_1$ is required. The magnitude of R_1 may be found by taking the scalar product of $\vec{R}_1$ with each term of 4-2:

$$R_1^2 = \vec{R}_1 \cdot \vec{R}_1 = \vec{R}_1 \cdot \vec{S} + \vec{R}_1 \cdot \vec{R}_2 \qquad B\text{-}1$$

Similarly, the scalar product of Equation 4-2 with $\vec{S}$ and $\vec{R_2}$ yield:

$$\vec{R_1} \cdot \vec{S} = S^2 + \vec{R_2} \cdot \vec{S} \qquad \text{B-2}$$

$$\vec{R_1} \cdot \vec{R_2} = \vec{R_2} \cdot \vec{S} + R_2^2 \qquad \text{B-3}$$

Combining:

$$R_1^2 = 2\vec{R_1} \cdot \vec{S} + R_2^2 - S^2 = 2(\hat{R}_1 \cdot \vec{S}) R_1 + (R_2^2 - S^2) \qquad \text{B-4}$$

Equation B-4 is a quadratic scalar equation for the magnitude of R_1 . Solving for R_1 :

$$R_1 = \hat{R}_1 \cdot \vec{S} \pm \sqrt{(\hat{R} \cdot \vec{S})^2 + (R_2^2 - S^2)} \qquad \text{B-5}$$

The two solutions correspond to the two intersections of the line with the sphere. This ambiguity will be treated later in the section. The quantity $\hat{R}_1 \cdot \vec{S}$ can be evaluated:

$$\hat{R}_1 \cdot \vec{S} = (\hat{R}_1)_x S_x + (\hat{R}_1)_y S_y + (\hat{R}_1)_z S_z$$
$$= -\frac{1}{\sqrt{l^2 + f^2}} \left\{ l S_x + F S_y \sin s/F + F S_z \cos s/F \right\} \qquad \text{B-6}$$

It is also convenient to define:

$$U = \pm \sqrt{(\hat{R}_1 \cdot \vec{S})^2 + (R_2^2 - S^2)} \qquad \text{B-7}$$

so that:

$$R_1 = (\hat{R}_1 \cdot \vec{S}) + U \qquad \text{B-8}$$

B.2 Error Analysis

The vector giving target location is $\vec{R_1}$ specified as $R_1 \hat{R}_1$ by Equations A-5 and B-8. Except that R_1 is computed by a different equation for the panoramic camera-radar combination from that for two cameras, the analysis is identical to that given in Appendix A. The values of $\hat{R}_1$ and $[\partial \hat{R}_1 / \partial w_j]$ can be taken from Appendix A. Only the $[\partial \hat{R}_1 / \partial w_j]$ must be recalculated and a slightly revised list of variables is needed to account for sensor 2 now being a radar unit. The new variable list is:

w_j , j = 1 to 12 are the same as in Appendix A.

w_{13} = R_2 , the radar range measurement.

The same consideration as described in Appendix A must be used when navigation measurements are treated, with respect to single or separate flights over the target area.

The foregoing list of quantities available in Appendix A, plus the values of $[\partial R_1 / \partial \nu_j]$ are needed for Equation B-9. In order to differentiate R_1 it is convenient to evaluate $[\partial(\hat{R}_1 \cdot \vec{S})/\partial \nu_j]$ and $[\partial U/\partial \nu_j]$ separately. They are:

$$\frac{\partial(\hat{R}_1 \cdot \vec{S})}{\partial \nu_j} = \left(\frac{\partial(\hat{R}_1)}{\partial \nu_j}\right) \cdot \vec{S} + \hat{R}_1 \cdot \left(\frac{\partial \vec{S}}{\partial \nu_j}\right) \qquad \text{B-9}$$

$$\frac{\partial U}{\partial \nu_j} = \frac{1}{U}\left[(\hat{R}_1 \cdot \vec{S}) \frac{\partial(\hat{R}_1 \cdot \vec{S})}{\partial \nu_j} + R_2 \frac{\partial K_2}{\partial \nu_j} - S \frac{\partial S}{\partial \nu_j}\right] \qquad \text{B-10}$$

In B-9, the first term is listed in Appendix A; only the scalar product needs to be carried out. The second term is only non-zero for $\nu_j = \nu_{4,5,6}$. The values of $[\partial R_1 / \partial \nu_j]$ can be tabulated:

$$\frac{\partial R_1}{\partial \nu_1} = -\left\{S_x + \frac{l(\hat{R}_1 \cdot \vec{S})}{(l^2+F^2)^{1/2}}\right\}\left\{1 + \frac{\hat{R}_1 \cdot \vec{S}}{U}\right\}\left\{\frac{1}{(l^2+F^2)^{1/2}}\right\} \qquad \text{B-11}$$

$$\frac{\partial R_1}{\partial \nu_2} = \left[S_x \sin(s/F) - S_y \cos(s/F)\right]\left[\frac{1}{(l^2+F^2)^{1/2}}\right]\left[1 + \frac{\hat{R}_1 \cdot \vec{S}}{U}\right]$$

$$\frac{\partial R_1}{\partial \nu_3} = -\left\{S_y\left[\sin(s/F) - (s/F)\cos(s/F)\right] + S_x\left[\cos(s/F) + (s/F)\sin(s/F)\right] + \frac{F(\hat{R}_1 \cdot \vec{S})}{(l^2+F^2)^{1/2}}\right\}\left\{\frac{1+\frac{\hat{R}_1 \cdot \vec{S}}{U}}{(l^2+F^2)^{1/2}}\right\}$$

$$\frac{\partial R_1}{\partial \nu_4} = -\left\{\frac{l}{(l^2+F^2)^{1/2}} + \frac{1}{U}\left[\frac{l(\hat{R}_1 \cdot \vec{S})}{(l^2+F^2)^{1/2}} + S_x\right]\right\}$$

$$\frac{\partial R_1}{\partial \nu_5} = -\left\{\frac{F\sin(s/F)}{(l^2+F^2)^{1/2}} + \frac{1}{U}\left[\frac{(\hat{R}_1 \cdot \vec{S})\, F\sin(s/F)}{(l^2+F^2)^{1/2}} + S_y\right]\right\}$$

$$\frac{\partial R_1}{\partial \nu_6} = -\left\{\frac{F\cos(s/F)}{(l^2+F^2)^{1/2}} + \frac{1}{U}\left[\frac{(\hat{R}_1 \cdot \vec{S})\, F\cos(s/F)}{(l^2+F^2)^{1/2}} + S_z\right]\right\}$$

$$\left\{\frac{\partial R_1}{\partial \nu_7}, \frac{\partial R_1}{\partial \nu_8}, \frac{\partial R_1}{\partial \nu_9}\right\}$$ see Appendix A

$$\frac{\partial R_1}{\partial \nu_{10}} = \left[\frac{S_y F\cos(s/F) - S_z F\sin(s/F)}{(l^2+F^2)^{1/2}}\right]\left[1+\left(\frac{\hat{R}_1\cdot\vec{S}}{U}\right)\right]$$

$$\frac{\partial R_1}{\partial \nu_{11}} = \left[\frac{S_z l - S_x F\cos(s/F)}{(l^2+F^2)^{1/2}}\right]\left[1+\left(\frac{\hat{R}_1\cdot\vec{S}}{U}\right)\right]$$

$$\frac{\partial R_1}{\partial \nu_{12}} = \left[\frac{S_x F\sin(s/F) - S_y l}{(l^2+F^2)^{1/2}}\right]\left[1+\left(\frac{\hat{R}_1\cdot\vec{S}}{U}\right)\right]$$

$$\frac{\partial R_1}{\partial \nu_{13}} = \frac{R_2}{U}$$

Since R_1 would be given, in an error analysis, and $\vec{S}$ is known, the value of U may be found from:

$$U = R_1 - \hat{R}_1\cdot\vec{S} \qquad \text{B-12}$$

thereby eliminating the ambiguity originally in the sign of U. The sets of derivatives given by equations here and in Appendix A yield the desired results for $[\partial\vec{R}_1/\partial\nu_j]$.

APPENDIX C

RADAR STEREO ERROR ANALYSIS

In Section 4, the format of the error analysis is laid out. The purpose of this appendix is to establish the form of the basic target location equations for radar stereo and to evaluate $[\partial(\bar{R}_i)/\partial w_j]$ for this case.

C. 1 Location Equations

Each radar sensor is assumed to be a side-looking system with no elevation measurement. The range measurement is usually the most accurate measurement, while the azimuthal position is within the spread of the antenna pattern, which is assumed here to be centered at a right angle to the flight line. Two measurements (a range and azimuth determination) from each radar sensor overdetermines the target position. A range from each sensor plus one azimuth angle will locate the target, then using the other azimuth angle would reduce the location error (azimuth error would be reduced approximately by $\sqrt{2}$). Therefore, the basic system will be chosen to use two ranges and one azimuth angle, and the values assigned to azimuth error will be assumed to take account of the factor of $\sqrt{2}$.

The required location equations are the equations of 2 spheres and a plane since two ranges are measured and the antenna beam is essentially planar; the intersection point being the target location. Referring to Figure 4. 1, Section 4, and writing the equations in sensor coordinates:

$$\begin{aligned} (R_i)_i^2 &= X_i^2 + Y_i^2 + Z_i^2 \\ (R_2)_i^2 &= (X_i - S_{x_i})^2 + (Y_i - S_{y_i})^2 + (Z_i - S_{z_i})^2 \\ X_i &= 0 \end{aligned} \qquad \text{C-1}$$

where subscript 1 means "measured in coordinates of sensor 1."

Rotating the coordinate system such that the new x axis is in the direction of the base x axis provides results directly in base coordinates, except for translation. (It is again convenient to assume the base coordinates are oriented with z being vertical at sensor 1, thus allowing earth curvature to be ignored for the error analysis.) The equations for spheres remain the same, except that quantities are now measured in translated base coordinates.

The transformation for X_1 is:

$$X_1 = X\cos\psi - Y\sin\psi \qquad \text{C-2}$$

where ψ = angle between flight direction at sensor station 1 and x axis of base system. The new equations are therefore:

$$\begin{aligned} R_1^2 &= X^2 + Y^2 + Z^2 \\ R_2^2 &= (X - S_x)^2 + (Y - S_y)^2 + (Z - S_z)^2 \\ A'X - BY &= 0 \end{aligned} \qquad \text{C-3}$$

where $A' = \cos\psi$, $B = \sin\psi$. These three equations can be solved for by simple algebra, giving:

$$X = B\,(R_1^2 - Z^2)^{1/2} \qquad \text{C-4}$$

$$Y = A'\,(R_1^2 - Z^2)^{1/2} \qquad \text{C-5}$$

$$Z = \frac{MS_z \pm CD}{E} \qquad \text{C-6}$$

where:

$$M = \frac{R_1^2 - R_2^2 + S^2}{2} \qquad E = C^2 + S_z^2 \qquad \text{C-7}$$

$$C = BS_x + A'S_y \qquad D = [R_1^2 E - M^2]^{1/2}$$

The plus and minus choice in the value of Z is due to the two possible intersections of the plane and two spheres. In the error analysis this will be resolved because target location is an input, in practice the two Z values would be sufficiently different as to be separable by approximate altitude measurement. (One intersection may well be above the sensors.)

For the error analysis, X, Y, Z must be differentiated with respect to each measured variable. In this case, the variables are:

$$\begin{aligned} \nu_1 &= R_1 & \nu_6 &= S_x \quad S_{zx} \\ \nu_2 &= R_2 & \nu_7 &= S_{1x} \\ \nu_3 &= \psi & \nu_8 &= S_{1y} \\ \nu_4 &= S_x \quad S_{zx} & \nu_9 &= S_{1z} \\ \nu_5 &= S_y \quad S_{zy} \end{aligned} \qquad \text{C-8}$$

The navigation variables $\nu_j\ (j = 4 \text{ to } 9)$ are treated just as in Appendices A and B, with respect to one or two flights over the target. Therefore, only derivatives with respect to variables 1 to 6 are required.

C. 2 Error Analysis

Differentiating Equations C-4 and C-5 for X and Y :

$$\frac{dX}{dv_j} = (R_1^2 - Z^2)^{1/2} \frac{dB}{dv_j} + B(R_1^2 - Z^2)^{-1/2}\left[R_1 \frac{dR_1}{dv_j} - Z \frac{dZ}{dv_j}\right] \qquad \text{C-9}$$

$$\frac{dY}{dv_j} = (R_1^2 - Z^2)^{1/2} \frac{dA'}{dv_j} + A'(R_1^2 - Z^2)^{-1/2}\left[R_1 \frac{dR_1}{dv_j} - Z \frac{dZ}{dv_j}\right] \qquad \text{C-10}$$

These expressions will be evaluated for particular j values after the dZ/dv_j values are derived.

The derivatives of A, B, C, D, E, and M are necessary to evaluate dZ/dv_j. These derivatives are listed below, with zero values omitted.

$$\frac{dA}{dv_3} = -B \quad , \quad \frac{dB}{dv_3} = A' \qquad \text{C-11}$$

$$\frac{dM}{dv_1} = R_1 \quad , \quad \frac{dM}{dv_2} = -R_2$$

$$\frac{dM}{dv_4} = S_x \quad , \quad \frac{dM}{dv_5} = S_y \quad , \quad \frac{dM}{dv_6} = S_z$$

$$\frac{dC}{dv_3} = A'S_x - BS_y \quad , \quad \frac{dC}{dv_4} = B \quad , \quad \frac{dC}{dv_5} = A'$$

$$\frac{dE}{dv_3} = 2C\frac{dC}{dv_3} \quad , \quad \frac{dE}{dv_4} = 2BC \quad , \quad \frac{dE}{dv_5} = 2A'C \quad , \quad \frac{dE}{dv_6} = 2S_z$$

$$\frac{dD}{dv_1} = \frac{R_1(E-M)}{D} \quad , \quad \frac{dD}{dv_2} = \frac{MR_2}{D}$$

$$\frac{dD}{dv_3} = \frac{R_1^2 C}{D}\frac{dC}{dv_3} \quad , \quad \frac{dD}{dv_4} = \frac{(R_1^2 BC - MS_x)}{D}$$

$$\frac{dD}{dv_5} = \frac{(R_1^2 A'C - MS_y)}{D} \quad , \quad \frac{dD}{dv_6} = \frac{S_z(R_1^2 - M)}{D}$$

In terms of the above:

$$\frac{dZ}{dv_j} = \frac{1}{E}\left\{M\frac{dS_z}{dv_j} + S_z\frac{dM}{dv_j} \pm C\frac{dD}{dv_j} \pm D\frac{dC}{dv_j} - Z\frac{dE}{dv_j}\right\} \qquad \text{C-12}$$

After all differentiation has been completed, no generality is lost in the error study if ψ is taken as $\psi = 0$. This can be done because no direction has been set for the x axis of the base coordinates. With this simplification:

$$A' = 1 \quad , \quad B = 0 \qquad \text{C-13}$$

The values of $\frac{dX}{dv_j}$, $\frac{dY}{dv_j}$, and $\frac{dz}{dv_j}$ may be tabulated. They are listed below, with zero values omitted. Values are found by substitution of C-11 and C-13 into Equations C-9, C-10, and C-12.

$$\frac{dX}{dv_3} = Y \qquad \text{C-14}$$

$$\frac{dY}{dv_i} = \frac{R_i}{Y} - \frac{z}{Y}\frac{dz}{dv_i} \quad ; \quad \frac{dY}{dv_j} = \frac{-z}{Y}\frac{dz}{dv_j} \quad , \qquad j = 2 \text{ to } 6$$

$$\frac{dz}{dv_1} = \frac{R_1}{E}\left\{S_x \pm \frac{S_y(E-M)}{D}\right\} \quad , \quad \frac{dz}{dv_2} = \frac{R_2}{E}\left\{-S_x \pm \frac{S_y M}{D}\right\}$$

$$\frac{dz}{dv_3} = \frac{S_x}{E}\left\{\pm\frac{S_y^2 R_1^2}{D} \pm D - 2S_y z\right\} \quad , \quad \frac{dz}{dv_4} = \frac{S_x}{E}\left\{S_x \pm \frac{S_y(-M)}{D}\right\}$$

$$\frac{dz}{dv_5} = \frac{1}{E}\left\{S_y S_x \pm \frac{S_y^2}{D}(R_1^2 - M) \pm D - 2S_y z\right\} \quad , \quad \frac{dz}{dv_6} = \frac{1}{E}\left\{M + S_x^2 \pm \frac{S_y S_x (R_1^2 - M)}{D} - 2S_y z\right\}$$

Throughout Equations C-14, the double valued character of $\pm$ causes doubled values in dz/dv_j. This ambiguity can be removed in the error analysis, since z is an input parameter. If it is noted that D appears with every plus-minus pair, the source of the ambiguity may be found, since D was solved for as a square root and arbitrarily called positive. For the error analysis, D can be defined equivalently by C-6, as:

$$(\pm D) = \frac{Ez - MS_x}{C} \qquad \text{C-15}$$

The expression $\pm D$ may be replaced by the equivalent form which will assign the proper sign to the quantity, without ambiguity. Substitution of the values of C, E and M, and algebra will simplify C-15 to:

$$(\pm D) = -\left[YS_x - ZS_y\right] \qquad \text{C-16}$$

Using Equation C-16, the solutions for dZ/dv_j are unique. Since

$$X = (R_i)_x \;, \quad Y = (R_i)_y \;, \quad Z = (R_i)_z \qquad \text{C-17}$$

the values of $d(\vec{R}_i)/dv_j$ are listed as Equation C-14, completing the derivation.

APPENDIX D

EFFECTS OF MULTIPLE COVERAGE OF A SINGLE TARGET

In many cases, several sensor records contain data on the location of a target. Since the target can be located with respect to one sensor by measurement of three independent quantities, it is both possible and often probable that excess or redundant measurements will be available. Redundant measurements can be used to increase target location accuracy by adjusting the measured quantities according to a criterion such as maximum likelihood.

Weighted least squares analyses are available in the literature which are concerned with adjustment of measurements for photogrammetric control extension. D. C. Brown's, Reference 8, report contains a relatively complete treatment of the theory of weighted least squares. The method presented there will be used as a basis for the treatment of adjustments given here.

The form of the least squares analysis can be forced to remain fixed, independent of what sensor combinations are used to locate the target, and how many sensor records contain information about the target. The problem can be reduced to one of writing the condition equations in proper form. In all cases, the condition equations will be written (using the same notation as in previous sections) as:

$$\vec{R}_1 = \vec{R}_2 + \vec{S} \qquad D\ 1$$

where $\vec{R}_1$ and $\vec{R}_2$ are vectors from two sensor stations to the target, and $\vec{S}$ is the navigation vector giving the location of sensor 2 with respect to sensor 1. Of course, all vectors must be specified in a common coordinate system, so that some vectors may first have to be transformed to the proper system before being used.

The first pair of stations provides one vector condition equation (e.g., 3 scalar equations). Each additional station provides another vector equation, since each such equation expresses the fact that the vector from one station intersects the vector from station 1, at the target.

In order to carry out the analysis with uncorrelated measurements, the form in which each vector is expressed depends on what sensor is considered, since the vector must be expressed in measured quantities. For example, the vector for a frame camera would be:

$$\vec{R_1} = \alpha \begin{bmatrix} x_F \\ y_F \\ f \end{bmatrix} \qquad \text{D-2}$$

where: x_F, y_F are film coordinates

f is focal length

α is a multiplier which is unknown, since the camera does not measure distance to a target

For a side-looking radar system, however, the vector would be:

$$\vec{R_2} = r \begin{bmatrix} \cos\sigma \\ \sin\sigma \cos E \\ \sin\sigma \sin E \end{bmatrix} \qquad \text{D-3}$$

where: r is the measured range

σ is the antenna squint angle (normally $\pi/2$ for side-looking)

E is the elevation antle (usually not measured)

These vectors are expressed in sensor coordinates, and would have to be transformed to earth coordinates by a matrix involving roll, pitch and yaw angles of the sensor.

The values of the quantities used would be measured values for all measured quantities, and estimates for unmeasured quantities. The estimates would be obtained from the basic location equations derived in the previous sections.

The weighted least squares analysis can be carried out by following the form given in Appendix A of Reference 8. Since the theoretical aspects of the analysis are well covered in the reference, only a partial treatment is given here, in order to indicate the use of these procedures with sensors other than cameras. A brief, simplified example is given. The simplest possible case of the use of redundant data will be treated, in order to show how sensors other than cameras can be used for target location.

The case to be described is target location by means of one vertical frame camera at one station, and a side-looking radar at a nearby station. Since the camera determines the direction of a vector and the radar determines a magnitude and one direction of a second vector, four quantities are known, so the target is overdetermined by one measurement. Navigation and orientation measurements could be included in the adjustment, but this only lengthens the equations without adding to the illustrative value of the example. Moreover, the orientation (roll, pitch, and yaw) angles can be set as zero, thus making all transformation matrices simply unit matrices. Wherever possible, the notation of Reference 8 will be used, so that comparisons can be made easily.

It will be assumed that an approximate target location has been found, so that rough values are available for all quantities. The first problem, then, is to write the condition equations. These are given above. The form of $\vec{R}_1$ and $\vec{R}_2$ is taken from Equation D-2 and Equation D-3. The condition equations, in vector form, are:

$$\alpha \begin{bmatrix} x_p \\ y_p \\ f \end{bmatrix} - r \begin{bmatrix} \cos\sigma \\ \sin\sigma \cos E \\ \sin\sigma \sin E \end{bmatrix} - \begin{bmatrix} S_x \\ S_y \\ S_z \end{bmatrix} = 0 \qquad \text{D-4}$$

In this equation, the components of $\vec{S}$ are assumed to be known, not to be adjusted, and therefore constant. Because of the assumptions of known orientation, no transformation matrices appear. The quantities to be adjusted can be separated into 2 groups; those measured quantities (x_j) whose weighted adjustments are to be minimized, and the unmeasured quantities (γ_k) which are adjusted with zero weight (called parameters). These are:

$$\vec{x} = \begin{bmatrix} x_p \\ y_p \\ f \\ r \\ \sigma \end{bmatrix} \qquad \vec{\gamma} = \begin{bmatrix} \alpha \\ E \end{bmatrix} \qquad \text{D-5}$$

Labelling measured or estimated values with a superscript zero, the vectors of correction values may be defined:

$$\begin{aligned} \vec{v} &= \vec{x} - \vec{x}^0 \\ \vec{\delta} &= \vec{\gamma} - \vec{\gamma}^0 \end{aligned} \qquad \text{D-6}$$

The 5 measured quantities are assigned weights which are inversely proportional to the variances of the measurements, and a variance matrix is written with the variance of the j th measurement as the jj th matrix element:

$$\sigma^{\circ} = \begin{bmatrix} \omega_1^{-1} & 0 & 0 & 0 & 0 \\ 0 & \omega_1^{-1} & 0 & 0 & 0 \\ 0 & 0 & \omega_2^{-1} & 0 & 0 \\ 0 & 0 & 0 & \omega_3^{-1} & 0 \\ 0 & 0 & 0 & 0 & \omega_4^{-1} \end{bmatrix} \qquad \text{D-7}$$

The condition equations (D-4) are linearized by expanding in a Taylor series about the measured values, keeping only linear terms. It is convenient to define:

$\vec{\epsilon}$ = the vector condition equation with measured values inserted in place of true values. (i th component is ϵ_i)

$$a_{ij} = \frac{\partial \epsilon_i}{\partial x_j} \quad , \quad b_{ik} = \frac{\partial \epsilon_i}{\partial r_k^{\circ}} \qquad \text{D-8}$$

A, B = matrices with elements a_{ij} , b_{ik}

The condition equation (D-4) may be written in linearized form as:

$$A\vec{v} + B\vec{\delta} + \vec{\epsilon} = 0 \qquad \text{D-9}$$

For the present case, the matrices A and B are:

$$A = \begin{bmatrix} \alpha^{\circ} & 0 & 0 & 0 & r^{\circ} \\ 0 & \alpha^{\circ} & 0 & -\cos E^{\circ} & 0 \\ 0 & 0 & \alpha^{\circ} & -\sin E^{\circ} & 0 \end{bmatrix}, \quad B = \begin{bmatrix} x_p^{\circ} & 0 \\ y_p^{\circ} & r^{\circ}\sin E^{\circ} \\ f^{\circ} & -r^{\circ}\cos E^{\circ} \end{bmatrix} \qquad \text{D-10}$$

Using the method of Lagrange multipliers, the weighted sum of squares of residuals is within:

$$S = \vec{v}^{T}(\sigma^{\circ})^{-1}\vec{v} - 2\vec{\lambda}^{T}(A\vec{v} + B\vec{\delta} + \vec{\epsilon}) \qquad \text{D-11}$$

where the vector of Lagrange multipliers is: $\vec{\lambda}^{T} = (\lambda_1, \lambda_2, \lambda_3)$ for this case.

The magnitude of S is to be minimized. This process is carried out by differentiating S with respect to each free variable (i.e., all v's and δ's). Each partial derivative is set equal to zero to obtain a minimum

of S . Differentiating D-11 and writing the results in matrix form gives:

$$(\sigma^2)^{-1}\vec{v} - A^T\vec{\lambda} = 0 \qquad \text{D-12}$$

$$B^T\vec{\lambda} = 0 \qquad \text{D-13}$$

where D-12 comes from differentiating with respect to $\vec{m}$ and D-13 from $\vec{\delta}$. For the example given, Equations D-9, D-12, D-13 represent a set of 10 equations (3 + 5 + 2) in 10 unknowns (5 m's, 2 δ's, 3 λ's) to be solved.

Since the purpose of this example is to outline the procedure to be used, rather than to solve a particular problem, the straightforward but extremely lengthy solution will not be completed. The methods of solution and error analysis can be found in Reference 1. All of the required matrices have been set up for the problem considered, thus showing how such a sensor combination as camera-radar would be treated.